Alma Mater Studiorum - Università di Bologna

Dottorato di Ricerca in
Automatica e Ricerca Operativa

ING-INF/04 Automatica

XXI Ciclo

Cooperative Teleoperation Systems

Rita Bacocco

Il Coordinatore	**Il Relatore**
Prof. Paolo Toth	Prof. Claudio Melchiorri

A.A. 2005-2011

Contents

To myself,
ai miei amici Parco Trenno e City Bike!

"Il rimedio migliore quando si é tristi" replicó Merlino,
cominciando ad aspirare e mandar fuori boccate di fumo, é "Imparare Qualcosa".
É l'unico che sia sempre efficace.
Invecchi e ti tremolano mani e gambe,
non dormi alla notte per ascoltare il subbuglio che hai nelle vene,
hai la nostalgia del tuo unico amore,
vedi il mondo che ti circonda devastato da pazzi malvagi,
oppure sai che nelle chiaviche mentali di gente ignobile il tuo onore viene calpestato.
In tutti questi casi vi é una sola cosa da fare: imparare.
Imparare perché la gente parla tanto e che cosa la fa parlare. É l'unica cosa che la mente non riesca mai ad esaurire,
mai ad alienare, mai ad esserne torturata, mai a temere o a diffidarne, mai a sognarsi di esserne pentita.
Imparare é il rimedio per te. Guarda quante cose ci sono da imparare!
La scienza pura - unica purezza esistente. Puoi passare l'intera vita a studiare l'astronomia, tre anni la storia naturale, sei la letteratura.
Poi dopo aver esaurito un milione di esistenze sulla biologia, la medicina, la critica teologica, la geografia, la storia e l'economia, puoi cominciare a costruire la ruota di un carro col legno adatto, oppure passare cinquant'anni a imparare come si comincia a battere il tuo avversario nella scherma.
Dopo di che puoi riprendere dalla matematica,
finché é tempo che impari ad arare la terra.

Terence H. White - The Once and Future King, C.P. Putnam's Sons, New York 1958.

Chapter 1

Introduction and Thesis Outline

This chapter addresses a survey of the cooperative teleoperation systems and an overview of the state-of-art systems in this field. Moreover, the subjects discussed in this thesis will be presented briefly, along with an outline of the work.

The Cooperative Teleoperation combines two traditional fields of robotics which are *Teleoperation* and *Collaborative Manipulation*.

Teleoperation, from Greek origin, is composed of the prefix *tele*, which means "at a distance" and *operation*, meaning perform a task. Thus teleoperation extends the human capability of manipulating an object at a distance by providing the operator similar conditions to those of a remote location. It has received great attention from the scientific community in the last 70 years (see Fig. 1.1) as it permits the interaction with enviroments which could be dangerous or inaccessible to human beings, achieving simple or complex tasks. Teleoperation has been used in different fields. These are space (see Fig. 1.2), underwater exploration, military operations (see Fig. 1.3), mining, toxic and nuclear material handling, the entertainment industry, and more recently in surgery and microsurgery (see Fig. 1.4).

The rapid development of the Internet has also given a relevant impulse to the gouwth of telerobotics since it represents a communication channel available everywhere which can put differents systems geographycally located all over the world into communication(see. [1], [2], [3]).

A classical teleoperator system is made up of a *master* device that is manipulated by the operator and a *slave* device which handles the remote environment, interconnected by a *communication channel*. The Teleoperator system is interfaced on one side with the *human operator* and on the other side with the *environment*. Usually, each master and

Figure 1.1: Ray Goertz, seen here operating a mechanical-link teleoperator, later invented the first electronic remotely operated manipulators. Source: Argonne National Laboratories.

slave device has its own local control system which permits the execution of a task.
Typically, in order to execute a task remotely the operator imposes a desired force/velocity to the teleoperation system (acting directly on the master robot) and receives back from the environment a velocity/force feedback (sensed by the slave robot).
If the slave robot tracks the master's motion and the force perceived from master robot tracks the slave's force then the system is called *transparent*, [4]. Transparency can be used as an index to evaluate the performance of the teleoperation system. Ideally, it would be desirable to have a system with zero inertia in free motion and infinite stiffness in contact with a stiff wall, [5]. Moreover, the force feedback reflected back on the master robot gives the operator information about the remote environment, yielding a sense of telepresence, i.e. the human feels physically present at the remote. The force feedback on the one hand increases the operator's handling ability, but on the other compromises the stability of the entire system in presence of time delays, introduced by the inevitable physical distance between the master and slave sites.

Therefore, in addition to transparency, the control should also guarantee the stability of the whole system with time delays, keeping into account that, if the network latency increases, the overall performance will be worse.
Various control strategies have been developed for classical systems, directed towards resolving these two conflicting problems and to overcome the delays' effects, see [7] for an overview. Anderson et al. [6], using the analogy between the mechanical/electric circuits,

Figure 1.2: ExoMars, will be employed the robotic exploration of Mars. It will be launched in 2016 and in 2018 on two Mars missions. Source: European Space Agency.

represent a teleoperator as a network and applying the scattering theory, have proved that the instability caused by time delay was due to non-passivity of the communication channel. They have proposed a control law that compensates these problems by modeling the communication media as a two port lossless network (ensuring passivity) where the stability of link is guaranteed independently of the time delays. Successively [8] have extended the passivity concept introducing the wave variables formalism, providing a tool to model the communication media where the stability is guaranteed for any amount of (constant) time delay. Wave variable transformation has also been used with varying time delays for teleoperation over the Internet, [9]. In addition, approaches that do not require passivity assumptions have also been proposed, see e.g. [10] and [11]. The robotics literature proposes several control architectures for conventional teleoperator but one can observe that even though many control methodology have been applied to this fields, nowadays there isn't an approach or optimal solution to resolve the conflicting problems which afflict this challanging field.

By means of *Collaborative manipulation* people can accomplish tasks more effictively than in individual operations. There are many human activities where a group of people have an advantage over a single person. Also an individual using both hands/arms performs better results than using a single hand/arm. At the same time multiple robots, by means of cooperation, can perform more useful tasks than a single-robot. Multi robot systems have been extensively employed in the production processes such as manufacturing and automotive application (assembling, transporting, painting and welding) where a large

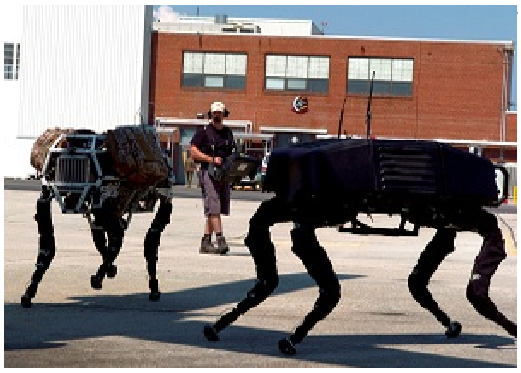

Figure 1.3: Big-dog-military-robots is the newest military transporter which can carry up to 120lbs and walks at the speed of up to 3.3 miles per hour. Source United States Departement od Defense.

manuverability, manipulability and flexibility are required (see Figure 1.5).
Thus with respect to conventional single-operator/single-robot manipulation, cooperative robotic manipulation can further facilitate task excution by enabling the collaboration among severeal operators or allowing bi-handed manipulation by a single operator. Moreover the cooperation has the advantages over single-robot to achieve results more efficiently, increasing dexterity and loading capacity, improving handling capability and enanching robustness due to the redundancy. In the cooperative manipulation multiarm robot manipulate a common object. These are very complex tasks where it is need analyses for them many control aspect. Extensive studies has been proposed in the past years by the robotics community addressed to resolve the problem of synchronization and coordination of multirobot systems, see e.g. [12], [13], [14], [15], [16], [17], [18] and many others.

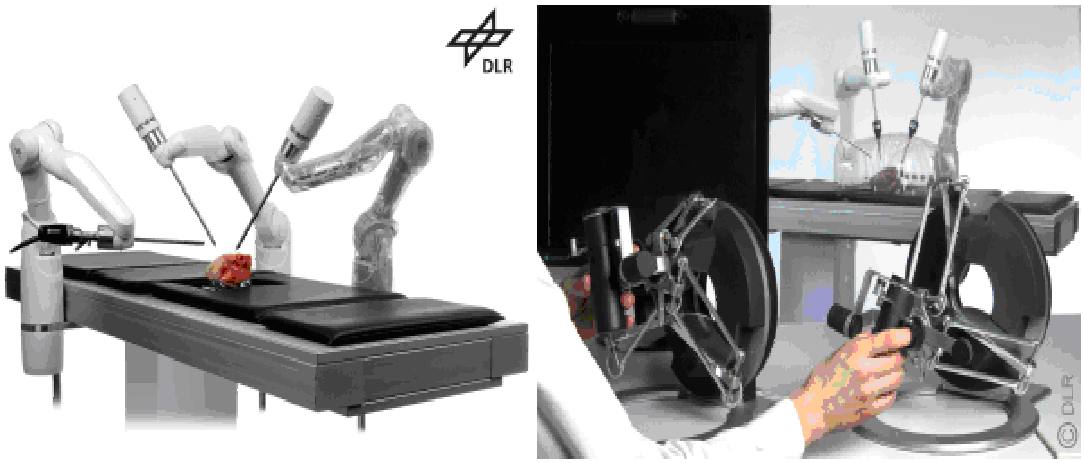

Figure 1.4: The DLR MiroSurge robotic system can be employed in minimally invasive robotic surgery. It consists of three MIRO robots, remotely commanded by a surgeon who comfortably sits at an input console. The surgeon virtually regains direct access to the operating field by having 3D endoscopic sight, force feedback, and restored hand-eye-coordination. Source DLR

Figure 1.5: FIAT assembly line. Source: espansioneonline. NewspaperMilano s.r.l

Cooperative teleoperation strung togheter the human manipulation skills with the robot precision and repeatability. The cooperative teleoperation systems are composed of more than one teleoperation device and permit the execution of a task at a distance from one or more operators located in the same or different place. The slave devices can interact directly or throug a common tool or by means the remote environment. It is necessary to guarantee stability and transparency for them as in the conventional systems.
In cooperative teleoperation the communication between the teleoperators conditions the choice of the control architectures. If the exchange of information is needed among the devices composing the system a centralized teleopeation control should be implemented, otherwise a decentralized approach is adequate.
Previous research activity on cooperation proposes multilateral communication frameworks with centralized controllers allowing information flow among all master and slave robot. In [19], [20], [21] controllers based on μ-synthesis methodology and adaptive techniques are introduced in absence of time delay, while in [22] a LQG algorithm optimized for trasparency is used considering constant time delays. Many works have been reported in the cooperative control of telerobot over the Internet. Goldenberg et al. [24] set up a collaborative teleoperated system in which through the developed client's Internet browser, several users can play a game together. Elhajj et al. [25] developed a multi-site Internet-based teleoperation system which allows operators from Hong Kong and Japan control the mobil manipulator located at USA cooperatively in real time. Chong et al. [26] built a tele-manipulation test bed in which one local opertaor and one remote operator control the robot with a local on-line graphics simulator. Kheddar et al. [27] developed along distance multi-robot teleoperation system between Japan and France using an intermediate functional representation of the real remote world by the means of virtul realty. Suzuki et al. [28], [29] designed a human interface system to control multi-robot using the World Wide Web. each robot in the system has its own ID number, and the operator is able to operate alll of them by using the developed interface system. [30] has developed a method of design and analysis of event synchronous systems based on Petri Net models for remote operation in multi-robot environments.

1.1 Outline

This thesis deals with the studies carried out by the author on the Cooperative Teleoperation Systems. The literature on cooperative teleoperation did not take into account control architectures composed of pairs of wave-based bilateral teleoperators operating in a shared environment. The author in her reasearch activity, introduces two cooperative control schemes based on wave variables by considering two pairs of single-master/single-slave devices collaborating to carry out operations in a shared remote environment. Such architectures have been validated both with simulations and experimental tests.
Ch. 2 introduces a description of the two control architectures proposed and presents some simulation results where the cooperative teleoperation systems evolve in free space and in contact with a stiff wall.
In the Ch. 3 some experimental results which confirm the positive results of the control schemes are illustred. Such results have been achieved by using a prototype custom built at *Laboratory of Automaiton and Robotics of University of Bologna*, which is also illustrated in this chapter.
In Ch. 4 the problem of defining proper tools and procedures for an analysis, and possibly a comparison, of the performances of cooperative teleoperation systems is addressed. In particular, a novel generalization of criteria adopted for classical (i.e. one master-one slave) teleoperators is presented and illustrated on the basis of the force-position and the position-position cooperative control schemes proposed in Ch. 2, both from a transparency and stability point of view, and by assuming a null time delay in the communication channel.
Ch. 5 collects final comments about the obtained results and the possible guidelines for future work.

Chapter 2

Cooperative Control Architectures

This chapter deals with two control architectures for cooperative teleoperation systems analised by the author in her research activity. In particular force-position and position-position architectures based on wave variables are presented and discussed. Moreover, various results obtained by means of the simulations with different time delays are carried out to prove the positive results of the two control schemes proposed.

In the cooperative teleoperation systems multiple operators, handling multiple teloperators, collaborate in order to accomplish a common task remotely. Usually the slave robots interact directly or by means of a common tool. However, the exchange of information may happen either between the corresponding pairs of single-master teleoperation robots, or between all robots which make up the system, see [21]. Cooperative teleoperation hasn't received much attention from the robotic community which makes it a completely open robotic field from a research point of view. The type of control proposed in the past on these systems consider architecures centralised, (see [19] and [22]), where there is a central unit to which the information regarding all devices making up the system arrives and from which leaves. The most relevant advantage of this type of control is the possibility to establish links between all master and slaves robots, improving the coordination in the cooperative teleoperation task. Another improvement is the exchange of information between two neighbor devices (i.e. between two slaves) reducing the time delays in the local communication channel with advantages both on stability and performance. The disadvantages are the use of a more complex communication system and bigger computational effort of the design process.
The cases studied propose decentralized architectures for cooperative teloeperation, see [31], where the computational effort is reduced, in fact each controller has a small number of state, input and output. The drawback of the scheme is that each slave device may

only receive the information from its corresponding master device but, on the other hand the number of signals to be transmitted is minimized.
The literature on cooperative teleoperation does not take into account control architectures composed of pairs of wave-based bilateral teleoperators operating in a shared environment. This work introduces two cooperative control schemes considering two pairs of single-master/single-slave devices working together in order to carry out operations in a remote environment. Stability and transparency are requested for them in the presence of the time delays in the communication channel. The main features of the proposed frameworks are:

- In each scheme, the information exchange only occurs between the corresponding pairs.
- The slave robots may physically interact among themselves through the tool and/or the remote environment.
- The stability of the system in the presence of time delay is ensured by applying concepts based on the passivity theory, thus modeling the communication channel by means of the wave variable transformation.
- The transparency of the control design is realized by a proper selection of the value of the wave impedance b.
- The master/slave devices of the same teleoperator are assumed kinematically similar.
- The dynamics of the manipulators and of the environment are known.

2.1 Description of the system

Figure (2.1) shows the basic cooperative architecture of the two proposed schemes. It is composed of two teleoperation systems interacting by means of a remote environment. Both systems are structured as a serial connection of two-port elements, including master-slave interconnected devices, each one interfaced on one side with the operator and on the other side with the shared environment.
It is well known that the interconnection of passive elements gives a passive system, see [6] for more details. This condition guarantees the stability of the teleoperation system when it interacts with arbitrary passive environments, see [32]. In this work, the master and slave devices are passive by construction, and are modeled with masses and dampers, and both the operator and the environment are assumed to be passive. Moreover, the communication channel with wave variables, guarantees passivity -and therefore stability- with respect to time delays. Finally, the control architecture of each teleoperator is designed

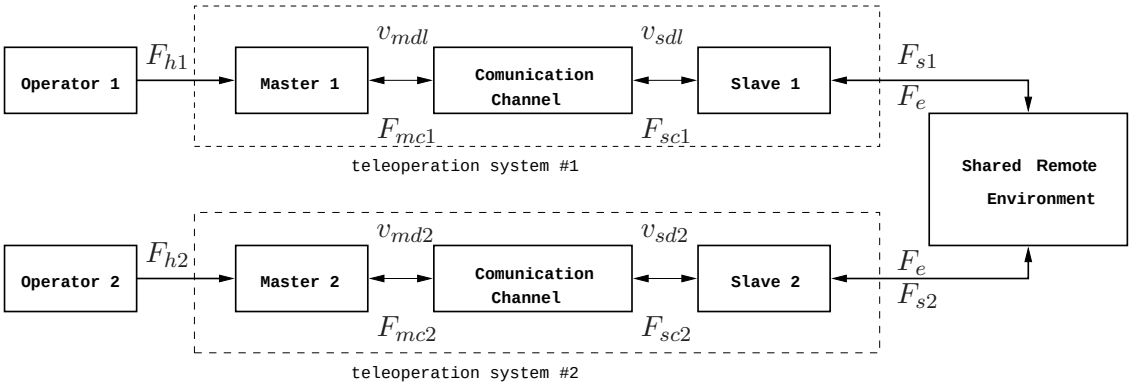

Figure 2.1: Structure of the system.

to be passive. These assumptions guarantee the overall stability of the system.
In the following, a brief survey of the wave-variables is given before the description of the two control architectures which are utilized to study the cooperative teleoperation.

2.1.1 Wave Variables and Passivity concept background

Both control schemes are based on a communication channel using wave variables. The wave-variables, are an extension or modification of the passivity theory which try to avoid the energy generation in a system, see [8].
Before introducing the wave-variables, some concepts on the passivity theory are reported. By modeling the communication channel which links the forces F_m and F_s to the velocities v_m and v_s of a teleoperator, as a two-port circuit as follow:

$$\begin{bmatrix} F_m(s) \\ \\ -v_s(s) \end{bmatrix} = \begin{bmatrix} h_{11}(s) & h_{12}(s) \\ \\ h_{12}(s) & h_{22}(s) \end{bmatrix} \begin{bmatrix} v_m(s) \\ \\ F_s(s) \end{bmatrix} \tag{2.1}$$

where $F_{m,s}(s)$ and $v_{m,s}(s)$ are the Laplace trasform of $F_{m,s}(t)$ and $v_{m,s}(t)$. In the presence of time delays the *Hybrid matrix*, see [33], which establishes the relations between the effort and flow of an ideal transparent bilateral teleoperation is given as:

$$H(s) = \begin{bmatrix} 0 & e^{-sT_d} \\ \\ -e^{-sT_d} & 0 \end{bmatrix} \tag{2.2}$$

The parameter T_d represents the time delay between the master and the slave devices. To prove the passivity of the comunication link with the time delays it is necessary to also introduce the *Scattering matrix* given as:

$$S(s) = \begin{pmatrix} 1 & 0 \\ 0 & 1 \end{pmatrix} * (H(s) - I) * (H(s) + I)^{-1}$$

Anderson [6] has proven that the *Scattering Matrix* corresponding to the *Hybrid matrix* eq. (2.2), has the scattering operator unbounded, thus the system cannot maintain stability and at the same time performs ideal transparency. The proposal made by Anderson to guarantee the stability maintainig the best possible transparency is to model the communication link as an ideal transmission line.
The *Hybrid* and *Scattering* matrices in this case are given as:

$$H(s) = \begin{bmatrix} tanh(sT_d) & sech(sT_d) \\ -sech(sT_d) & tanh(sT_d) \end{bmatrix} \tag{2.3}$$

$$S(s) = \begin{bmatrix} 0 & e^{-sT_d} \\ e^{-sT_d} & 0 \end{bmatrix} \tag{2.4}$$

This choice makes the system passive, since the norm of its scattering matrix is equal to one, thus intrinsically stable. Based on this theory the communication law which makes the communication channel with time delay passive (as it is derived from the scattering matrix of a passive system) is given as:

$$\begin{aligned} F_{md}(t) &= F_s(t - T_d) + v_{sd}(t - T_d) + v_m(t) \\ v_{sd}(t) &= v_m(t - T_d) - F_s(t) + F_{md}(t - T_d) \end{aligned} \tag{2.5}$$

where

$$F_{md}(t) = F_s(t - T_d) \quad v_{sd}(t) = v_m(t - T_d)$$

The wave variables are an alternative energy-based tool to model the communication-channel and as is it well known, the wave variables transformation ensures passivity of communication blocks for arbitrary time delays. The wave variables are a pair of variables (u,v) which are defined based on the standard power variables ($\dot{x}$,F), by the following transformation:

$$u = \frac{b\dot{x} + F}{\sqrt{2b}} \qquad v = \frac{b\dot{x} - F}{\sqrt{2b}} \tag{2.6}$$

where the forward moving wave u encodes the velocity command $\dot{x}$ and the returning wave v generates the force feedback signal F.
The passivity of comunication block is tested in the time domain, with zero initial energy stored by showing that the output energy of the communication block is less or equal to the input energy for all times:

$$\begin{aligned} E(t) &= \int_0^t P(\tau)d(\tau) = \int_0^t (P_{in}(\tau) - P_{out}(\tau))d(\tau) \\ &= \int_0^t F^T(\tau)(\dot{x(\tau)})d(\tau) \geq 0 \end{aligned} \tag{2.7}$$

In the wave domain eq. (2.7) becomes:

$$\int_0^t (\frac{1}{2}u_l^T u_l - \frac{1}{2}v_l^T v_l - \frac{1}{2}v_r^T v_r + \frac{1}{2}u_r^T u_r)d(\tau) \geq 0 \tag{2.8}$$

where the subcripts l and r indicate the left and right wave according to Fig. 2.2. By considering the following links due to the communication channel:

$$v_r(t) = u_l(t - T_d) \quad v_l(t) = u_r(t - T_d) \tag{2.9}$$

Substituting eq. (2.9) into eq. (2.8) it is shown that all power is stored according to:

$$E_{store}(t) = \int_a^t (\frac{1}{2}u_l^T u_l + \frac{1}{2}u_r^T u_r)d(\tau) \geq 0 \tag{2.10}$$

where a is equal to $t - T_d$. The wave energy is thus temporarily stored while the wave u_l and u_r are in transit making the communication link which is not only passive but also lossless. This is independent of the time delay from which the knowledge is not requested, see [34].

Shown in Fig. 2.2 is the communication channel based on wave variables where, in place

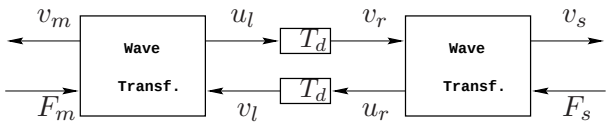

Figure 2.2: Wave-based architecture.

of the power variables $v_{m/s}$ and $F_{m/s}$ (velocity and force), the wave variables $u_{l/r}$ and $v_{l/r}$ are transmitted across the communication link. The transformation between power and wave variables is given by

$$\begin{aligned} u_l(t) &= \tfrac{1}{\sqrt{2b}}(F_m + bv_m), \qquad & u_r(t) &= \tfrac{1}{\sqrt{2b}}(F_s - bv_s) \\ v_l(t) &= \tfrac{1}{\sqrt{2b}}(F_m - bv_m), \qquad & v_r(t) &= \tfrac{1}{\sqrt{2b}}(F_s + bv_s) \end{aligned} \tag{2.11}$$

where b is the characteristic wave impedance which directly affects the behavior of the system. Depending on the choice of the input/output pairs traveling the comunication channel, it is possible to make four different wave transformations to which corrispond four different architectures. These architecures which are well known in literature are position-force, (i.e. position control at the master side and force control at the slave side), position-position, force-position and force-force. Among these architectures, this work considers the cases which the slave devices are under position control, i.e position-position *admittance-type* and force-position control or *hybrid-type*.

2.1.2 Architecture of the control schemes

In this thesis, the subscripts m and s denote the variables of the master and slave manipulators respectively, the subscript $i = 1, 2$ indicate the two teleoperators. The two control schemes described differ in the control strategies utilized on each pair of teleoperators. One is position-position (PP) control (i.e. both the master and slave of the two teleoperators are under position control), see Fig. 2.3, the other is force-position (FP), see Fig. 2.4. In both frameworks the devices under position control are regulated with a local PD controller whose gains have been obtained solving an optimal LQ problem.

In each teleoperator the considered master/slave devices are a single-degree-of-freedom (DOF) with dynamic model given by

$$M_{mi}\dot{v}_{mi} + B_{mi}\dot{x}_{mi} = F_{mi} \tag{2.12}$$

$$M_{si}\dot{v}_{si} + B_{si}\dot{x}_{si} = F_{si} \tag{2.13}$$

where v_{mi} and v_{si} are the velocities for the master and slave, x_{mi} and x_{si} are the positions, M_{mi} and M_{si} are the inertias, B_{mi} and B_{si} are the damping coefficients. F_{mi} and F_{si} are the forces applied on the master and slave devices respectively and are given as

$$F_{mi} = F_{hi} - F_{mcd} \tag{2.14}$$

$$F_{si} = F_{sci} - F_e \tag{2.15}$$

where F_h and F_e are, respectively, the forces exerted by the operator and by the environment, and F_{sc} is the force computed by the slave controller.
The value of F_{mcd} depends on the kind of control architecture. In the position-position control scheme, the force F_{mcd} is computed by the master controller and is equal to F_{mc}, see Fig. 2.3. In the force-position control scheme, F_{mcd} is the force which comes directly from the communication channel, coded with the wave variable, i.e. F_{md}, see Fig. 2.4 and Table 2.1. The remote environment has been modeled as mass-spring-damper system whose dynamics is described as

$$M_e\dot{v}_e + B_e\dot{x}_e + K_e x_e = F_{se_1} + F_{se_2} \tag{2.16}$$

with

$$\begin{aligned} F_{se_1} &= k_c(x_{s1} - x_e), \\ F_{se_2} &= k_c(x_{s2} - x_e) \end{aligned} \tag{2.17}$$

where v_e, x_e are the velocity and position of the environment. M_e, B_e, K_e represent the inertias, damping and stiffness coefficients of the environment, respectively. F_{se_1} and

Wave Trasf.	Master Side	Slave Side
Position-position	$v_{mdi} = \frac{1}{b}(\sqrt{2b}v_{li} + F_{mci})$ $u_{li} = \frac{1}{\sqrt{2b}}(\sqrt{2b}v_{li} + 2F_{mci})$	$v_{sdi} = \frac{1}{b}(\sqrt{2b}v_{ri} - F_{sci})$ $u_{ri} = \frac{1}{b}(bv_{ri} - \sqrt{2b}F_{sci})$
Force-position	$F_{mdi} = bv_{mi} - \sqrt{2b}v_l$ $u_{li} = (\sqrt{2b}v_{mi} - v_{li})$	$v_{sdi} = \frac{1}{b}(\sqrt{2b}v_{ri} - F_{sci})$ $u_{ri} = \frac{1}{b}(bv_{ri} - \sqrt{2b}F_{sci})$

Table 2.1: Wave-variables transformations for position-position and force-position architecture.

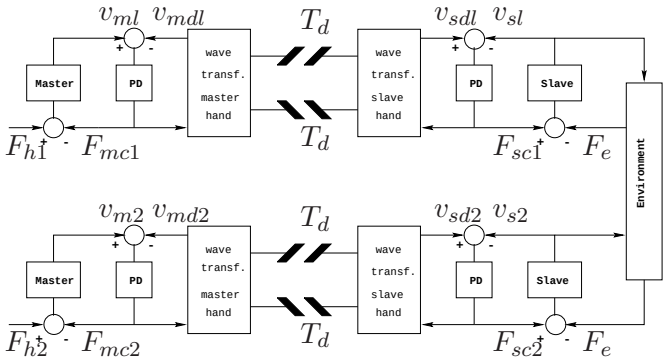

Figure 2.3: Wave based position-position control architecture.

F_{se_2} are the forces exerted on the remote environment by each slave device. The spring k_c takes into account the contact between the slave robots and the common tool (of slave-tool interaction).

Table 2.1 depicts the relations between the forces, velocities and the forward and returning waves for both position-position and force-position schemes. Such equations have been directly computed by the wave transformations eq. (2.11), see [35].

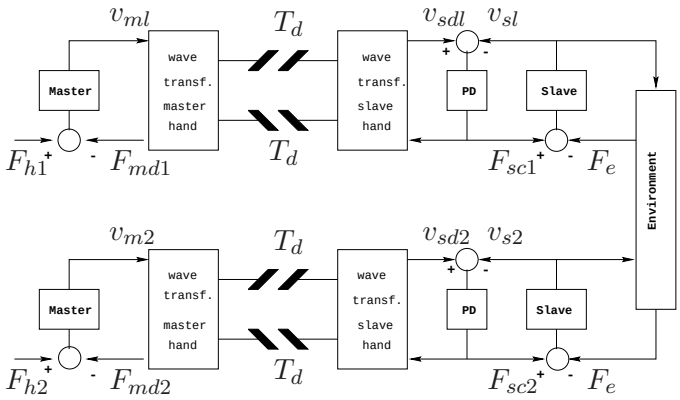

Figure 2.4: Wave based force-position control architecture.

2.1.3 Control Design

The robots under position control in the two telemanipulation systems have been controlled by standard PD controllers, whose parameters have been properly tuned with an optimal approach. The LQ synthesis technique has been adopted both in the force-position architecture (to compute the gains of the slave controllers), and in the position-position scheme (to compute the gains of both master and slave controllers). In the proposed implementation, a desired velocity command $v_{mdi}/_{sdi}$ is generated by means of an input force and tracked using a PD controller given by

$$F_{mci/sci} = K_P(x_{mi/si} - x_{mdi/sdi}) + K_D(v_{mi/si} - v_{mdi/sdi}) \tag{2.18}$$

where $x_{mi/si}$ is the master/slave position and $x_{mdi/sdi}$ is the desired position of the devices.

As it is well known, the LQ control problem involves the minimization of a cost functional as

$$J = \int_0^\infty (x^T Q x + u^T R u) dt \tag{2.19}$$

where u is the input, x the state of the system, and $Q > 0$ and $R > 0$ two proper matrices. The solution of the LQ problem is the optimal control $K = [K_P,\ K_D] = -R^{-1}(B^T P)$, where $P > 0$ is the solution of the *Riccati* equation

$$A^T P + PA - PBR^{-1}B^T P + Q = 0$$

Gains	Master1/Slave1	Master2/Slave2
K_P	109.5445 $[N/m]$	109.5445 $[N/m]$
K_D	6.2133 $[Ns/m]$	8.7406 $[Ns/m]$

Table 2.2: Gains of PD controllers

2.2 Simulation results

In order to verify the efficiency of the proposed schemes in terms of performance and stability, a system with two teleoperators has been simulated in the execution of two different tasks. In both tasks, two users act remotely applying a force (F_{h1}, F_{h2}) on their master devices. The slave manipulators, by means of a shared tool/object m_t, impose such forces on the environment, characterized by a stiffness k_e and a damping coefficient b_e.

The numerical values of the parameters used in the simulations are the following: $m_{m1} = 0.2$ $[kg]$, $b_{m1} = 0.5$ $[Ns/m]$, $m_{m2} = 0.4$ $[kg]$, $b_{m2} = 0.7$ $[Ns/m]$, $m_{s1} = 0.2$ $[kg]$, $b_{s1} = 0.5$ $[Ns/m]$, $m_{s2} = 0.4$ $[kg]$, $b_{s2} = 0.7$ $[Ns/m]$, $F_{h1} = 10$ $[N]$, $F_{h2} = 10$ $[N]$, $m_t = 5$ $[kg]$, $b_e = 200$ $[Ns/m]$, $k_e = 10000$ $[N/m]$ and $k_c = 10000$ $[N/m]$. Note that different values for the masses of the two teleoperators have been considered. Table 2.2 lists the values of the PD controllers obtained by the setting $Q = [12000, 0; 0, 1]$ and $R = I$.

2.2.1 Pushing a common object

The first task is schematically illustrated in Fig. 2.5. The two slave devices initially are in free motion, then push the common object (a tool) by applying on it two forces along the same direction. The slaves push the object until it comes in contact with the environment (a rigid wall).

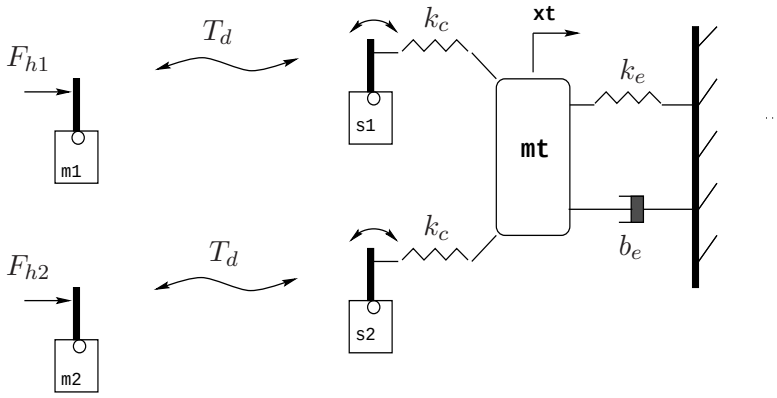

Figure 2.5: Task 1: the slave manipulators push a tool.

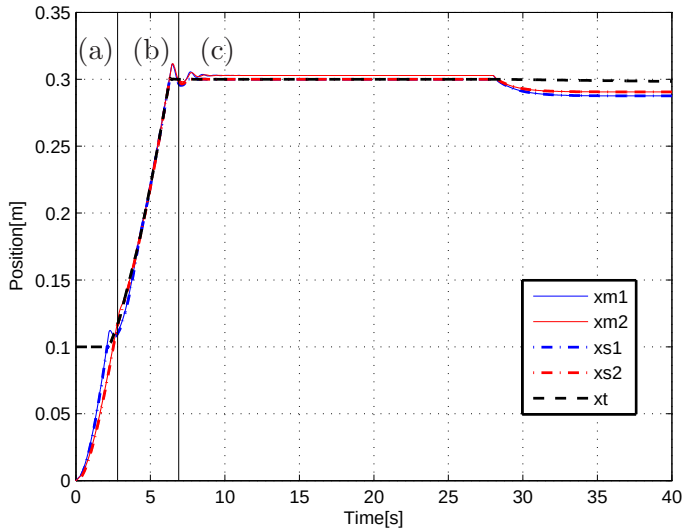

Figure 2.6: Task 1: position tracking with T_d=100 [ms]; (a) free motion; (b) contact with object; (c) contact with rigid wall (Position-Position).

Figure (2.6) shows, for the time delay $T_d = 100\ [ms]$, the position tracking between the master and slave devices of the corresponding pair in the three phases of the task: the free motion (a), in contact with the object (b), and when the object encounters the stiff wall (c). In particular, see Fig. 2.6, each slave, e.g. x_{s1} (dashdot line), tracks the behavior of its master x_{m1} (solid line) and evolves in free motion until contact with the tool positioned to $x_t = 0.1\ [m]$ occurs. After the contact, the tool begins to move, $x_t > 0.1\ [m]$ (dashed line), pushed only by the first slave, that results faster than the second one since it has a lower mass. When also the second slave reaches the tool ($x_t = 0.15\ [m]$), it helps the first one pushing it until contact with the environment placed at $x_t = 0.3\ [m]$ is made. The trajectory of the tool closely follows the position profiles of the slaves devices until the contact with the environment is made. Then obviously it stops, as expected, see x_t. Figure (2.7) illustrates the good force tracking of the operators' force, $F_{h1} + F_{h2}$ (dashdot line), by the force exerted by the object on the environment F_t (solid), after that the tool is in contact with the wall ($x_t = 0.3\ [m]$).

Figures (2.8) and (2.9) show the operator-environment and master-sleve force tracking profiles beetween each pair of two teleoperator. As can be noted from these figures each teleoperator shows good force tracking performaces.

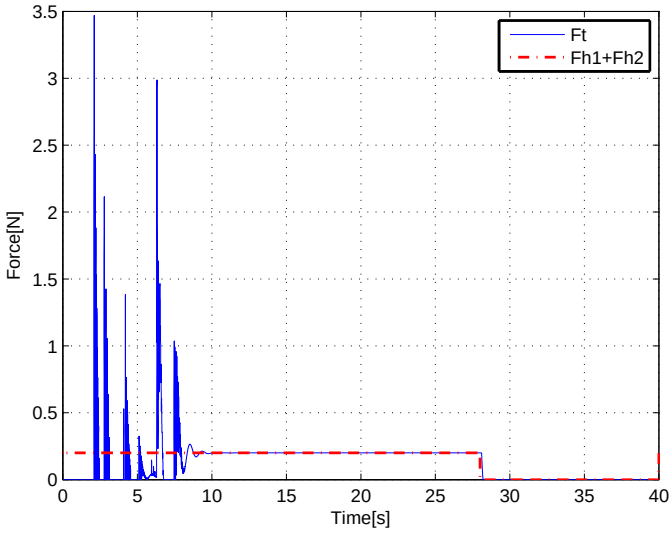

Figure 2.7: Task 1: force tracking with T_d=100 [ms] (Position-Position).

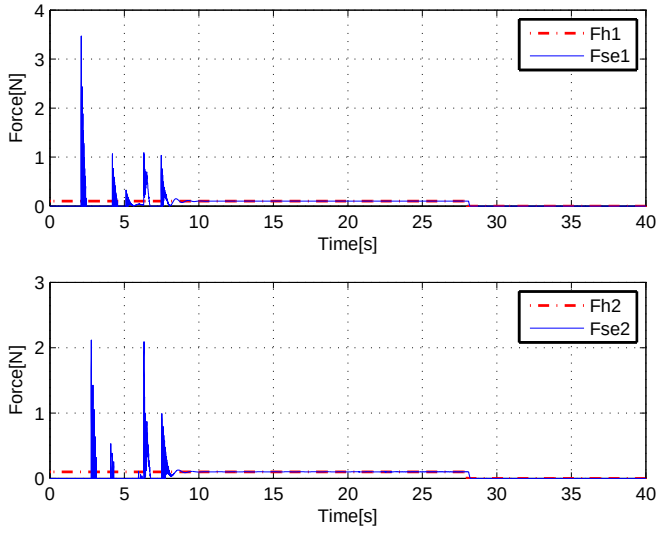

Figure 2.8: Task 1: force tracking profiles operator-environment with T_d=100 [ms] (Position-Position).

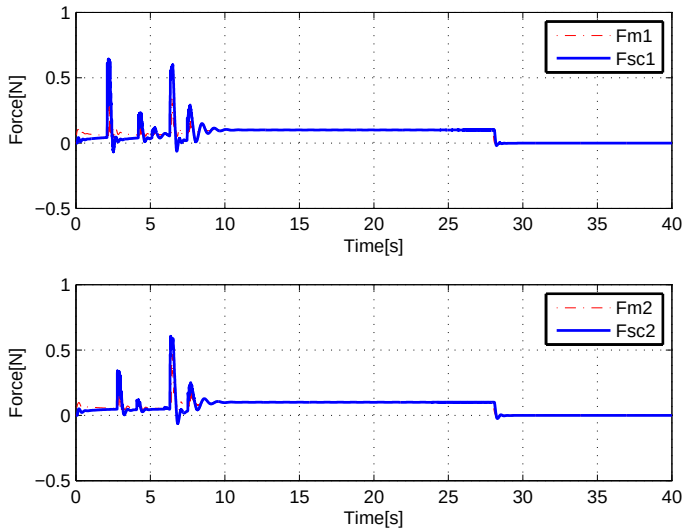

Figure 2.9: Task 1: force tracking profiles master-slave devices with T_d=100 [ms] (Position-Position).

Figures (2.10), (2.11), (2.12) and (2.13) show the results of the same task with time delay $T_d = 250\ [ms]$. Also in this case the tracking performances are guaranteed. The trajectory of the tool, instead, follows the position profile of the first slave until interaction with the second manipulator occurs. Then, it tracks the second slave, while the first one looses the contact. This behavior is due to the choice of the simulation parameters. In order to guarantee the transparency of the architecture, in both simulations ($T_d = 100,\ 250\ [ms]$) the wave impedance b has been set to 10 $[Ns/m]$.
Similar consideration can be made for FP algorithm which results are depicted in this section.

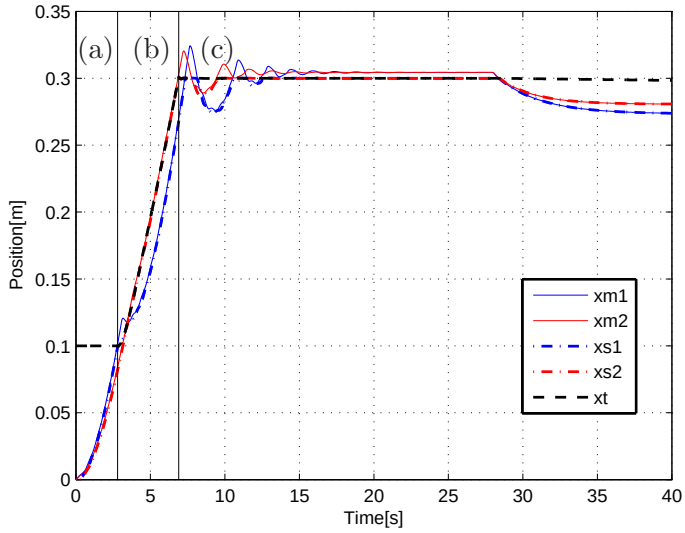

Figure 2.10: Task 1: position tracking with T_d=250 [ms]; (a) free motion; (b) contact with object; (c) contact with rigid wall (Position-Position).

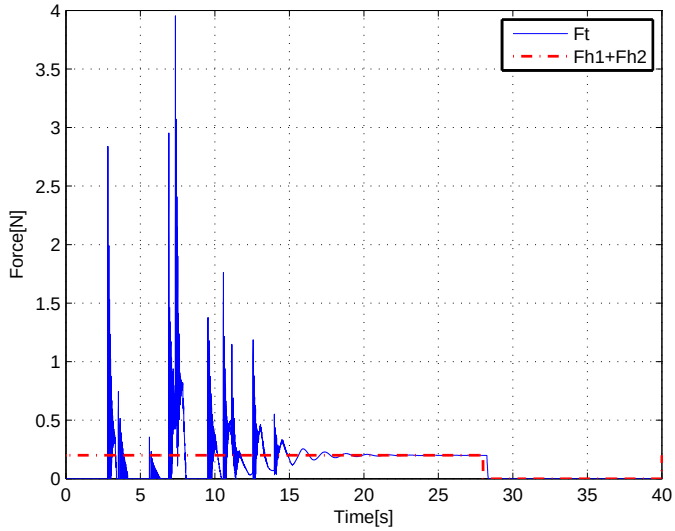

Figure 2.11: Task 1: force tracking with T_d=250 [ms] (Position-Position).

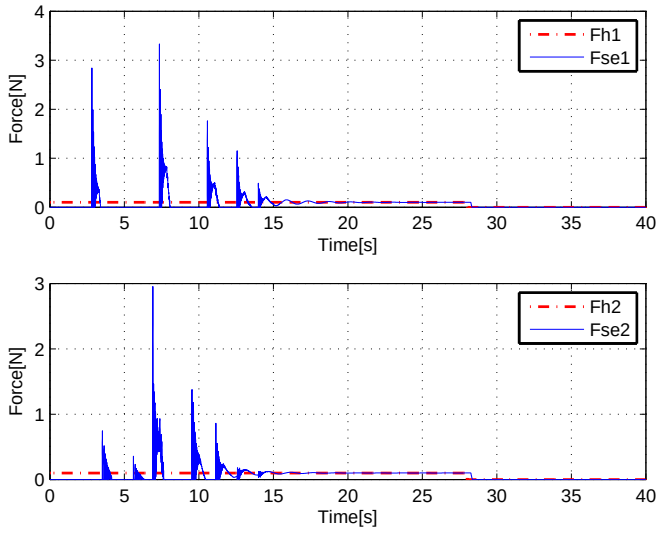

Figure 2.12: Task 1: force tracking with T_d=250 [ms] (Position-Position).

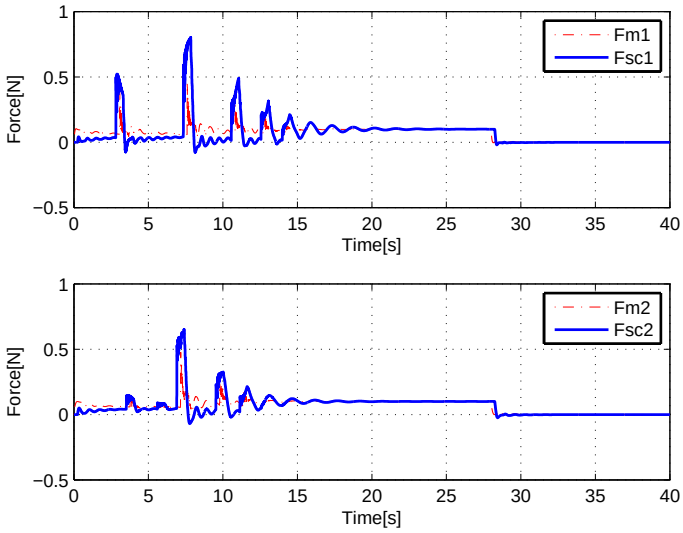

Figure 2.13: Task 1: force tracking with T_d=250 [ms] (Position-Position).

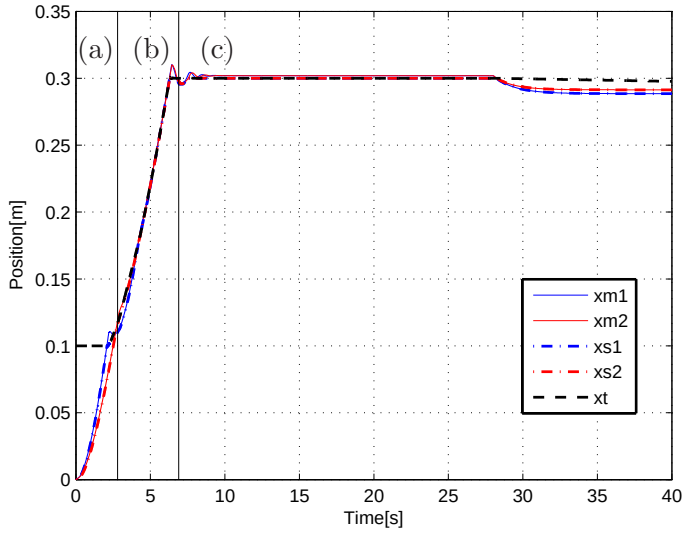

Figure 2.14: Task 1: position tracking with T_d=100 [ms]; (a) free motion; (b) contact with object; (c) contact with rigid wall (Force-Position).

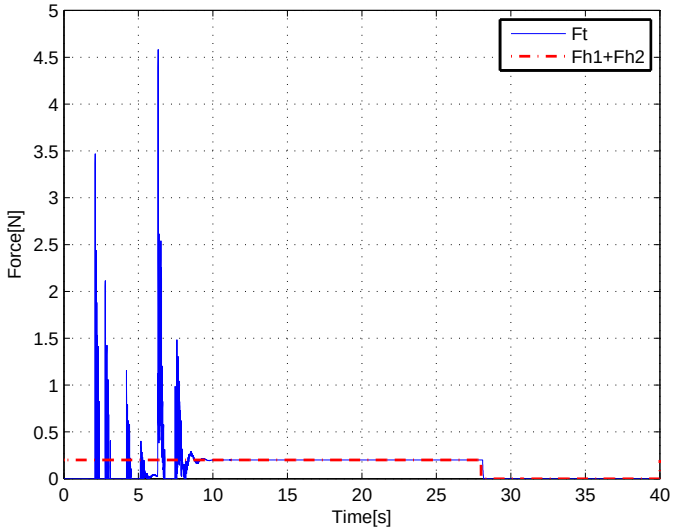

Figure 2.15: Task 1: force tracking with T_d=100 [ms] (Force-Position).

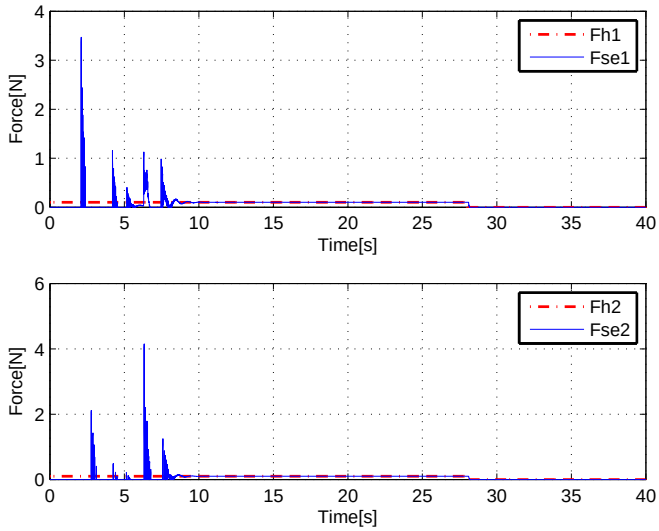

Figure 2.16: Task 1: force tracking with T_d=100 [ms] (Force-Position).

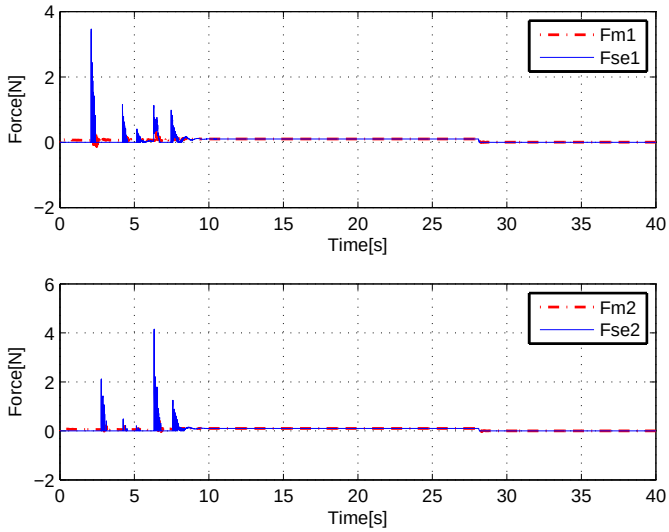

Figure 2.17: Task 1: force tracking with T_d=100 [ms] (Force-Position).

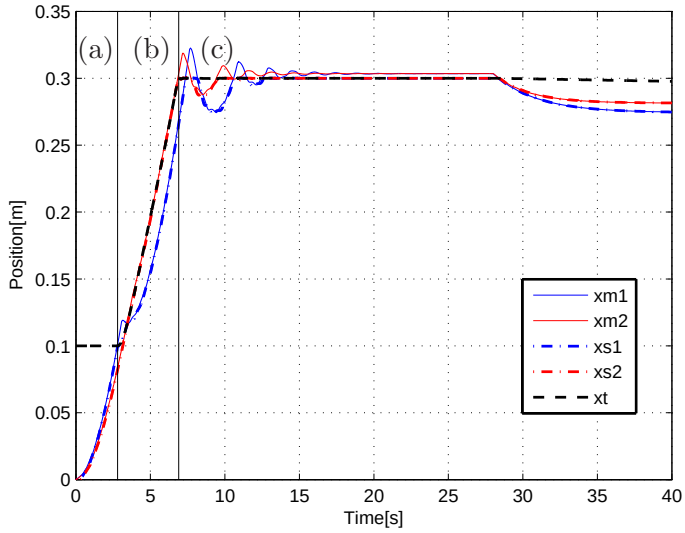

Figure 2.18: Task 1: position tracking with T_d=250 [ms]; (a) free motion; (b) contact with object; (c) contact with rigid wall (Force-Position).

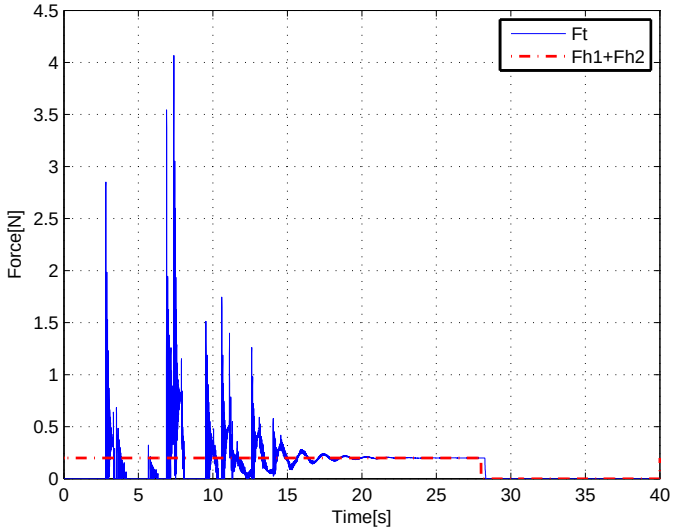

Figure 2.19: Task 1: force tracking with T_d=250 [ms] (Force-Position).

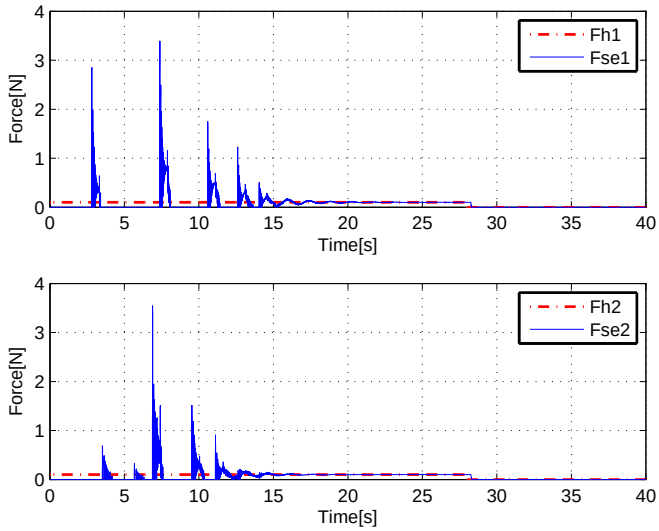

Figure 2.20: Task 1: force tracking with T_d=250 [ms] (Force-Position).

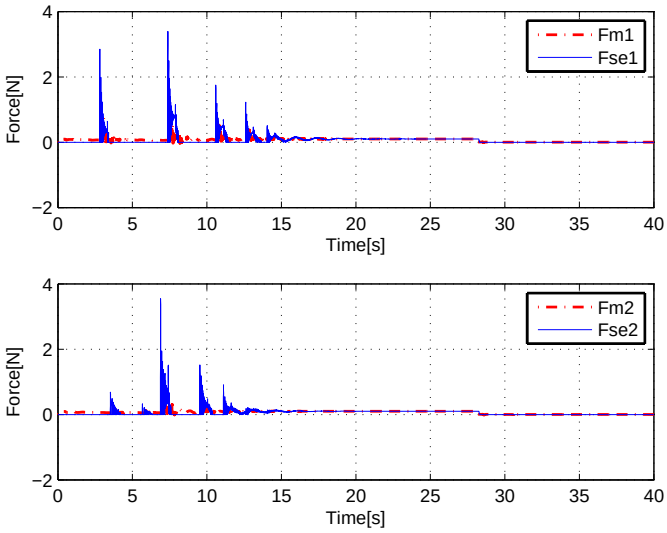

Figure 2.21: Task 1: force tracking with T_d=250 [ms] (Force-Position).

By comparing Fig. 2.6, Fig. 2.7, Fig. 2.8 and Fig. 2.9 with Fig. 2.14, Fig. 2.15, Fig. 2.16 and Fig. 2.17 it is possible to note how the tracking performances for force-position architecture is as good as the position-position one. However, in free motion tasks the force profiles of force-position architecture are worse than position-position because there is a larger number of oscillations causing the worsening of the users sensibility, see Fig. 2.7 and Fig. 2.15. This difference is emphasized for increased time delay as results from a comparison of Fig. 2.11 and Fig. 2.19 show.

2.2.2 Cooperative handling of an object

In the second task, the slave manipulators grasp and move an object by applying forces of different amplitudes on it, see Fig. 2.22. In this case the values $k_e = 0$, $b_e = 0$ and $m_{m1} = m_{m2}$ have been considered.
In this second task the object's mass is $m_t = 0.5$ $[Kg]$.

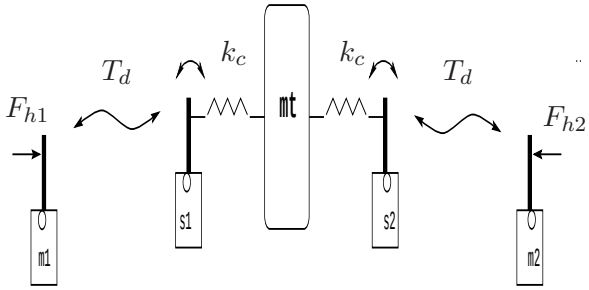

Figure 2.22: Task 2: the slave manipulators hold the tool.

Fig. 2.23 depicts the good position tracking between the master and slave devices, when the forces shown in Fig. 2.24 are imposed. Fig. 2.23 also shows the motion of the object, see x_t, that results accelerated or decelerated depending on the relative amplitude of the forces F_{h1} and F_{h2}.
In this task the system has good performances until 250$[ms]$, after that the stability is not guaranteed, as is shown in Fig. 2.25. Fig. 2.26 shows the position profiles of the devices when the slave manipulators move the object back and forth, by applying on it the forces reported in Fig. 2.27. In this case the system has a stable behaviour until 130$[ms]$, see Fig. 2.28 and Fig. 2.29. The Figures mentioned above are referred to the simulation results for a PP cooperative implementation. To complete the simulation results, the figures with the same tests for the force-position scheme of Fig. 2.4 are reported here. By comparing the two architectures you can note the similarities in the first test, see Fig. 2.23 and Fig. 2.25 with Fig. 2.30 and Fig. 2.31. In the second, FP shows instability starting from 110$[ms]$ see Fig. 2.33, while PP begins to work badly at 120$[ms]$, see Fig. 2.28 and shows distinct instability at 130$[ms]$, see Fig. 2.29. You can thus deduct that PP holds stability and transparency for longer time delays. This is due to the presence of the master controller in the PP control scheme.

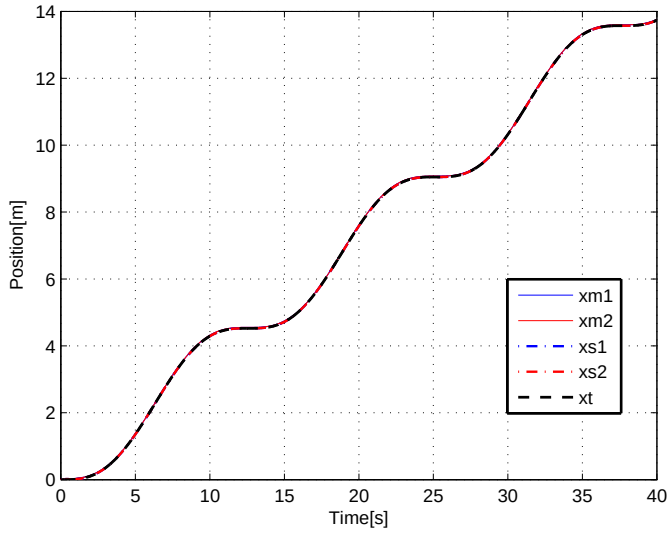

Figure 2.23: Task 2: position tracking with T_d=100 [ms] (Position-Position).

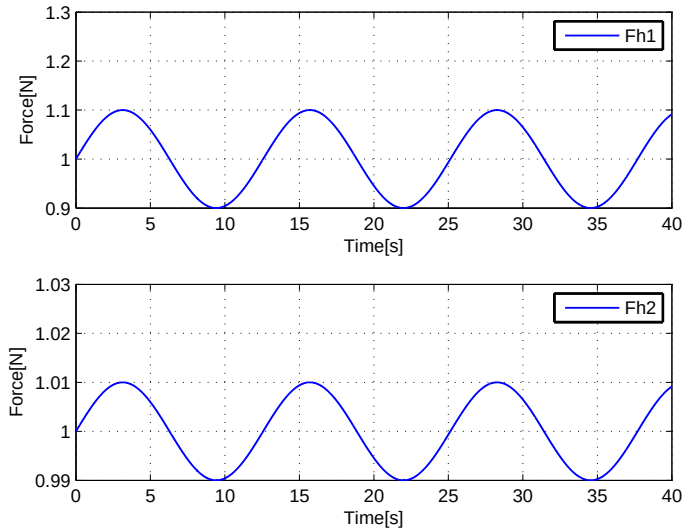

Figure 2.24: Task 2: Input force exerted by each operator. T_d=100 [ms] (Position-Position).

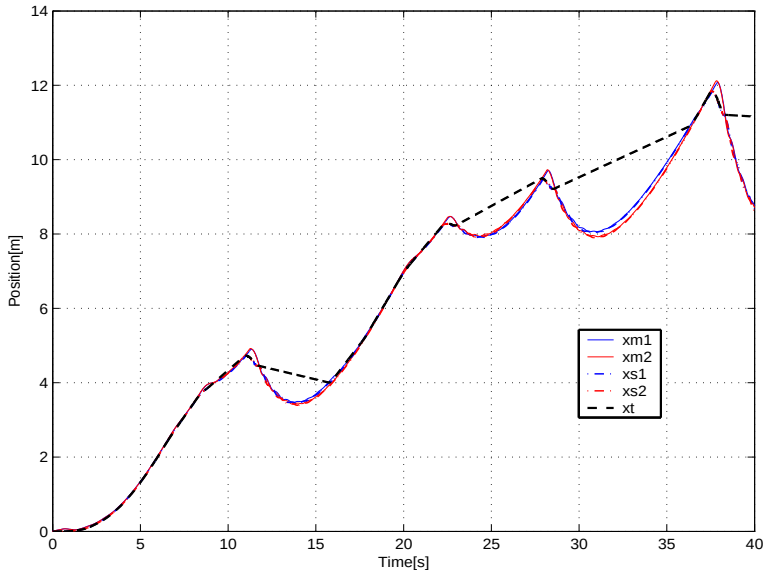

Figure 2.25: Task 2: position tracking with T_d=100 [ms] (Position-Position).

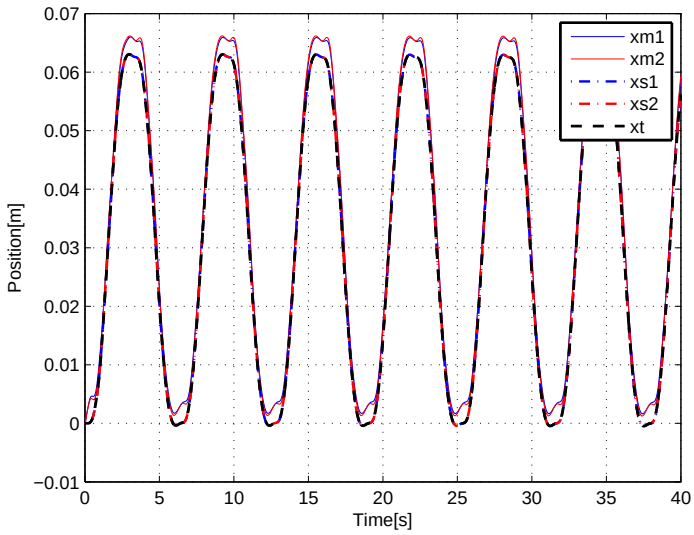

Figure 2.26: Task 2: position tracking with T_d=100 [ms] (Position-Position).

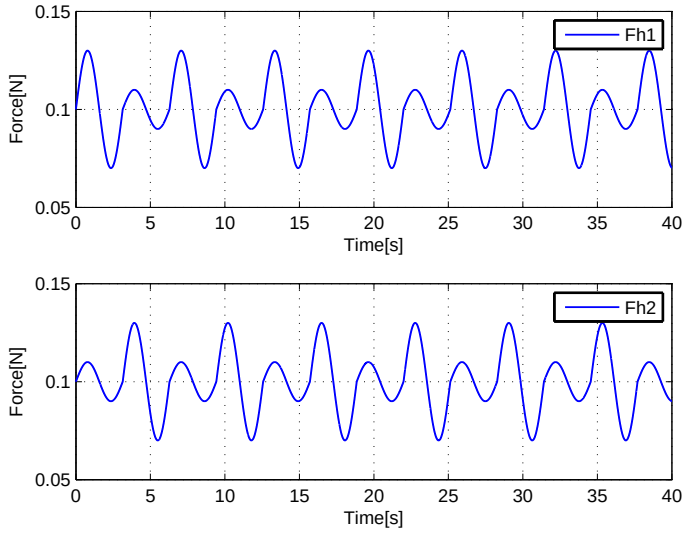

Figure 2.27: Task 2: Input force exerted by each operator. T_d=100 [ms] (Position-Position).

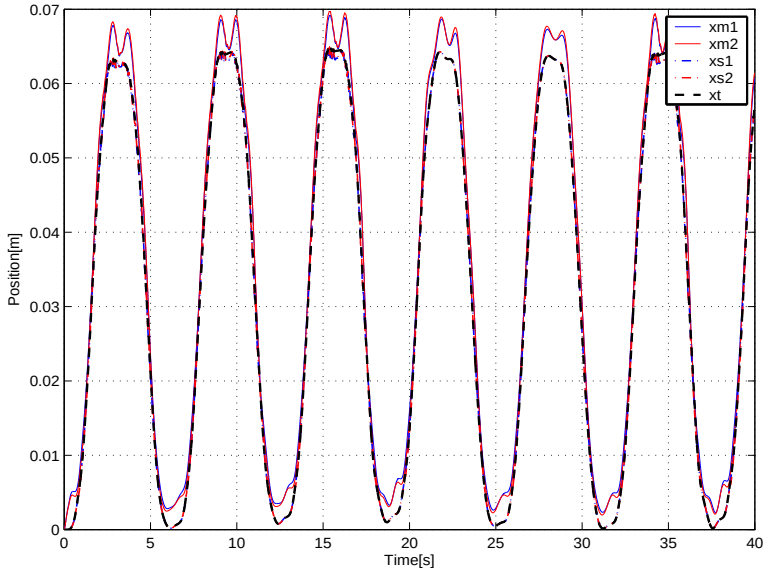

Figure 2.28: Task 2: position tracking with T_d=120 [ms] (Position-Position).

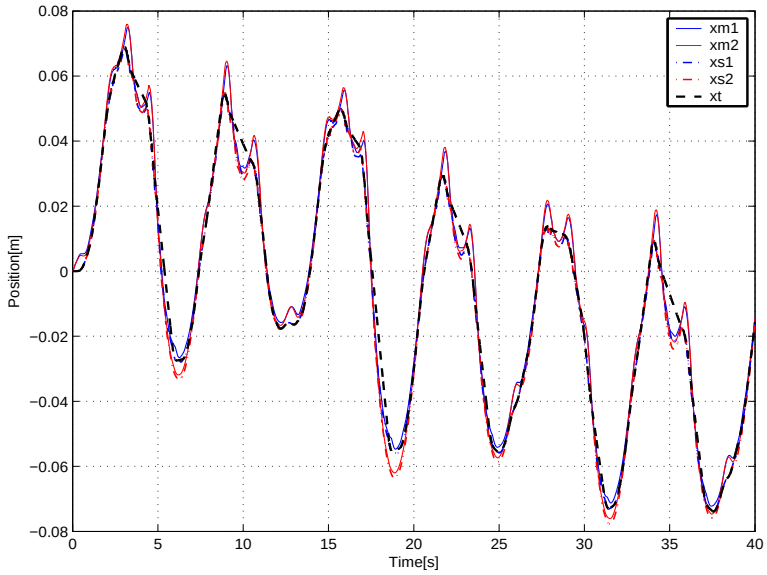

Figure 2.29: Task 2: position tracking with T_d=130 [ms] (Position-Position).

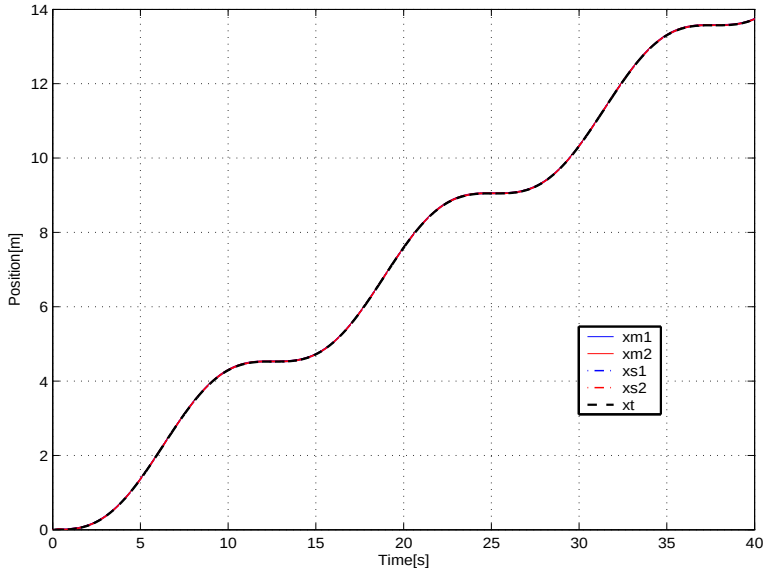

Figure 2.30: Task 2: position tracking with T_d=100 [ms] (Force-Position).

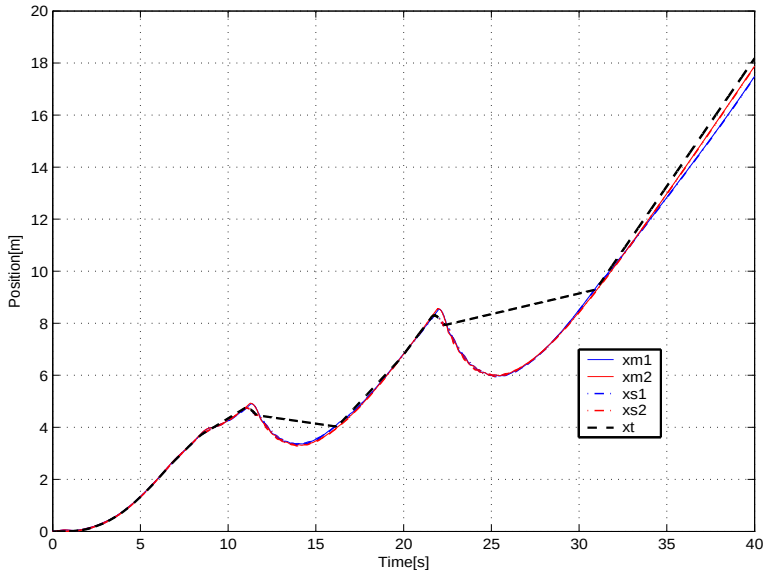

Figure 2.31: Task 2: position tracking with T_d=250 [ms] (Force-Position).

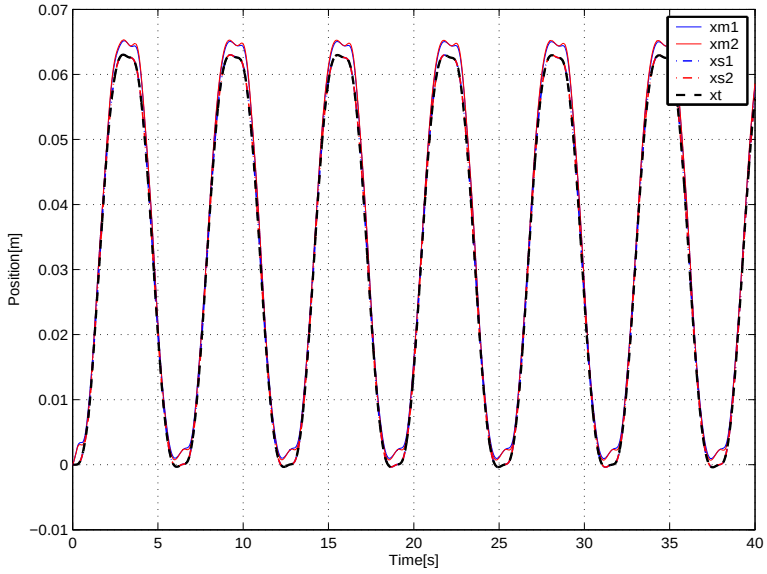

Figure 2.32: Task 2: position tracking with T_d=100 [ms] (Force-Position).

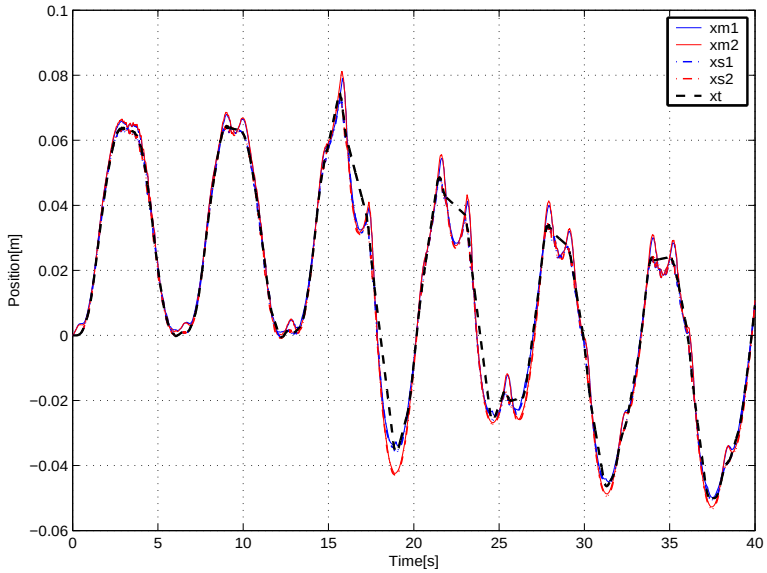

Figure 2.33: Task 2: position tracking with T_d=110 [ms] (Force-Position).

Chapter 3

Experimental Results

This chapter performs the experimental evaluation of the architecures proposed in Ch. 2. Some tests are reported and discussed in order to validate the performances of the control schemes under studies according to the simulation results. The evaluation has been done on a cooperative teleoperator system realized at *L.A.R.*. A brief description of the set up is reported.

3.1 Description of the Physical System

The experimental evaluation of the proposed schemes, see [36], has been performed with a cooperative teleoperation system built at *L.A.R.* (Laboratory of Automation and Robotics of University of Bologna) composed of two 1-DOF teleoperator systems, see Fig. 3.1. The prototype is based on four linear motors LinMot P01-23Sx80 with the servo controller LinMot E210-VF. The motors are equipped with position encoders with a resolution of 1 m, and high sensitivity load cells are placed on the top of the motor sliders. The control is implemented on a Pentium IV PC equipped with a Sensoray 626 data acquisition board. The OS is RTAI-Linux based on a Debian distribution, with Linux kernel 2.6.17.11 patched with RTAI 3.4. The real time I/O support for the acquisition board is provided by the Comedi drivers. The sample period for the digital controller and the D/A and D/A operations is 1msec. The control design has been developed within the Matlab/Simulink and Real Time Workshop environments, while the experimental data have been monitored with xrtailab.
For experimental evaluation of the two control schemes, the same tests made for simulation's evaluation have been repeated in the laboratory, see Sec. 2.2.

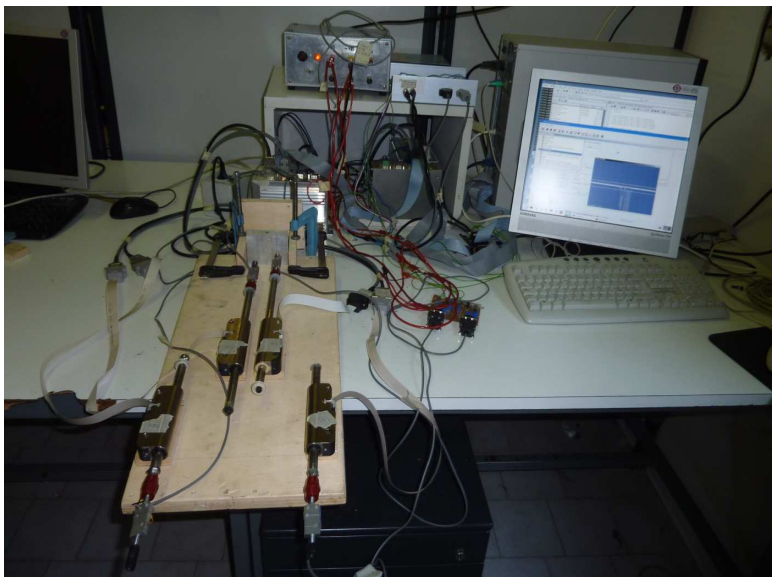

Figure 3.1: Cooperative manipulator, setup to push a common object.

3.2 Push a common object

In this task the user pushes the two masters forward and the two slave robots begin to move in free motion until the contact with the common tool is made. After that, the two slaves push the tool and a contact is made with a wall. This stops the tool and which consequently stops the two teleoperators. Figure (3.2) shows the positions of two master and slave devices for PP teleoperation systems with the time delay of $T_d = 100[ms]$. As can be noted, the two slave devices (red line) are initially in free motion and follow the motion of the masters (blue) until contact with the common tool ($x_t = 0.01[m]$) is made. The second slave starts pushing the tool which begins to move (see x_{s2}). When the second slave reaches the tool both of them push it together to the wall ($xe = 0.04[m]$), then both the slave devices are stopped as well as the corresponding masters. The force profiles Fig. 3.3 report the force tracking after the contact with the tool (approx. $0.5[N]$). Figures (3.4) and (3.5) illustrate the same profiles for the FP scheme. As can be deducted from these figures, the position tracking performances for the two architectures are similar. However FP shows a superior force tracking performance compared to PP, as for the bilateral systems, see [35], [37], [38] and [39] for more details. Similar considerations can be made for Fig. 3.6, Fig. 3.7, Fig. 3.8 and Fig. 3.9 which illustrate the same test with time delay of $T_d = 250[ms]$.

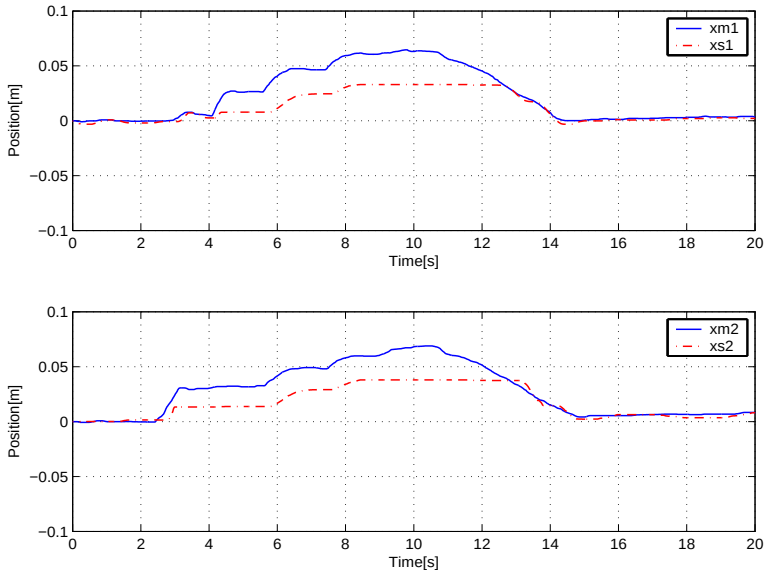

Figure 3.2: Task 1: position profiles with T_d=100 [ms] (Position-Position).

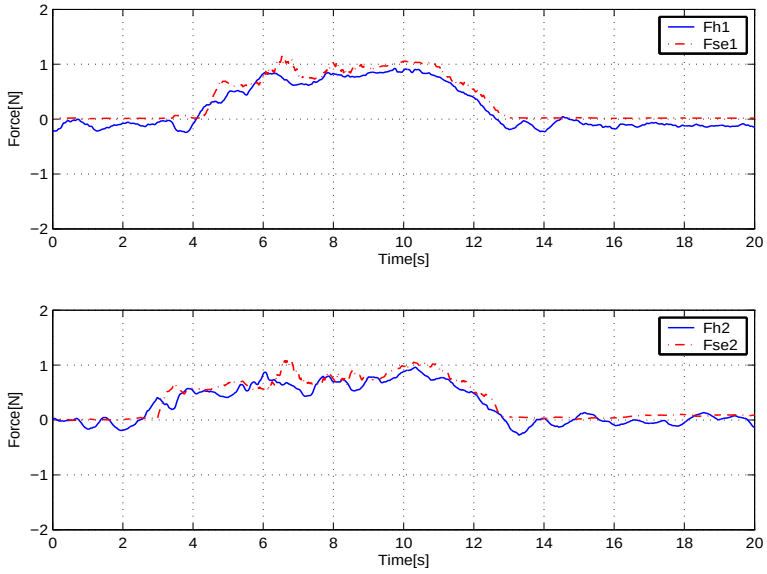

Figure 3.3: Task 1: force profiles with T_d=100 [ms]. Position-Position

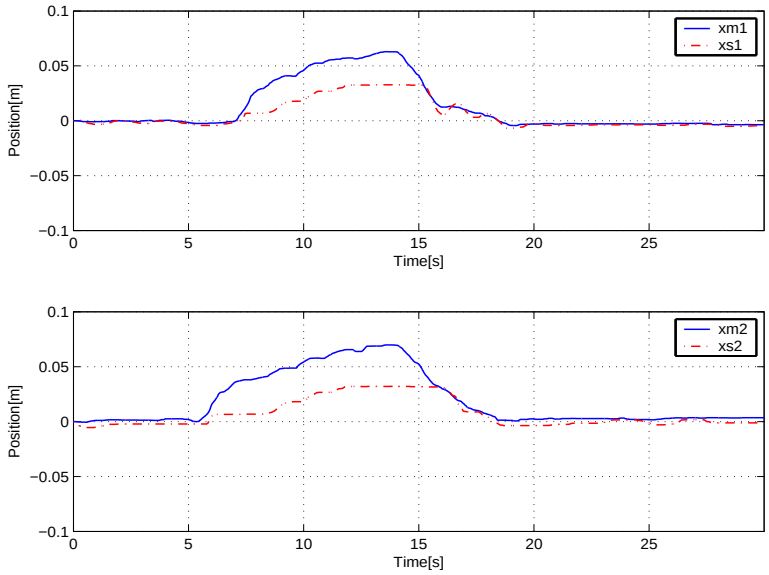

Figure 3.4: Task 1: position profiles with T_d=100 [ms] (Force-Position).

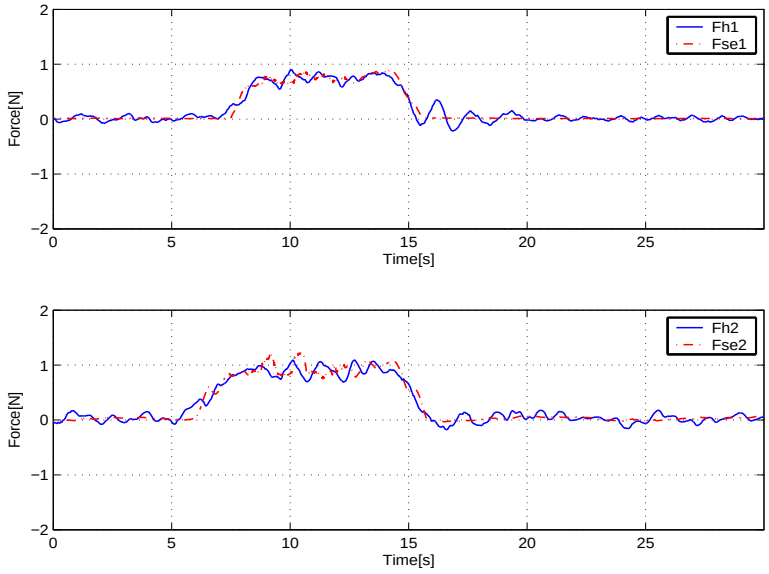

Figure 3.5: Task 1: force profiles with T_d=100 [ms] (Force-Position).

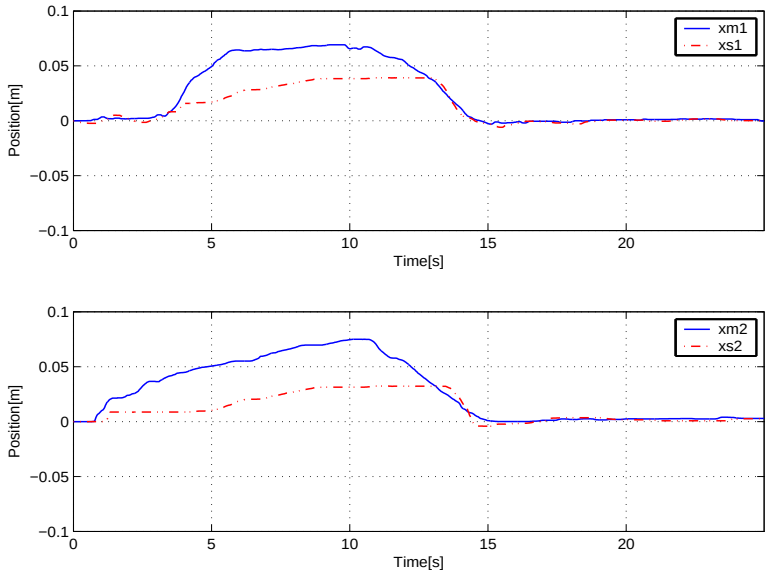

Figure 3.6: Task 1: position profiles with T_d=250 [ms] (Position-Position).

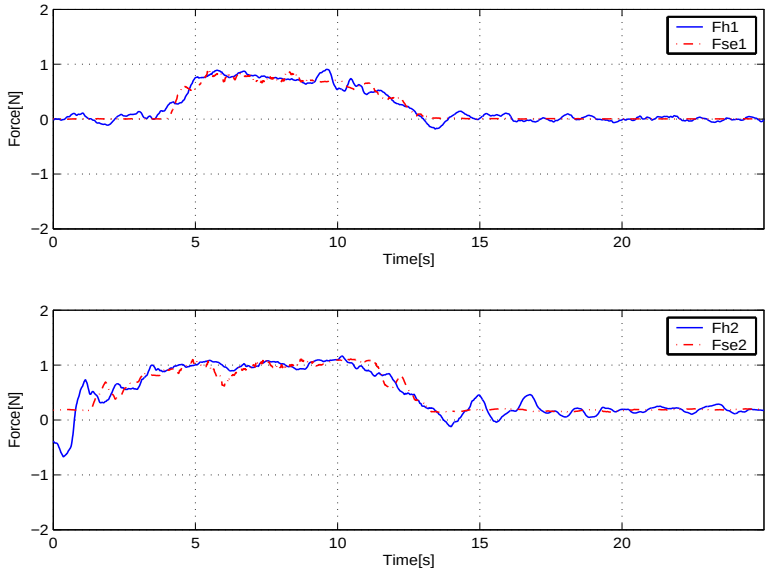

Figure 3.7: Task 1: force profiles with T_d=250 [ms] (Position-Position).

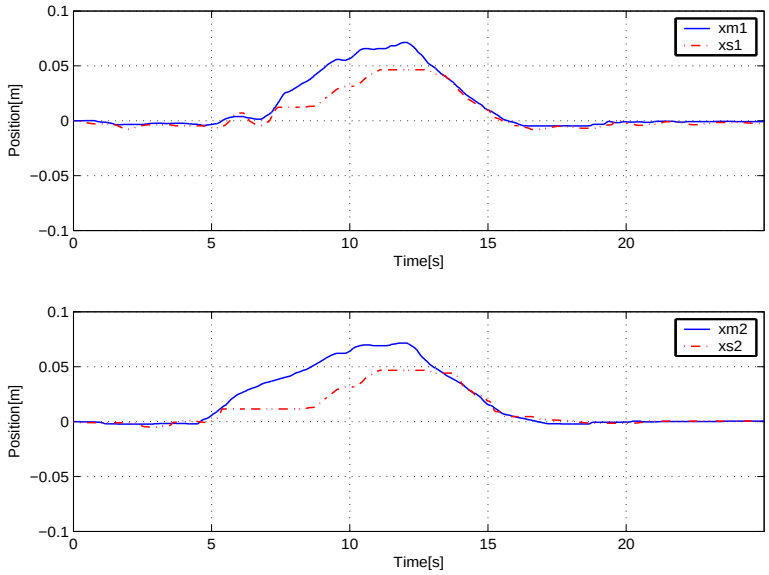

Figure 3.8: Task 1: position profiles with T_d=250 [ms] (Force-Position).

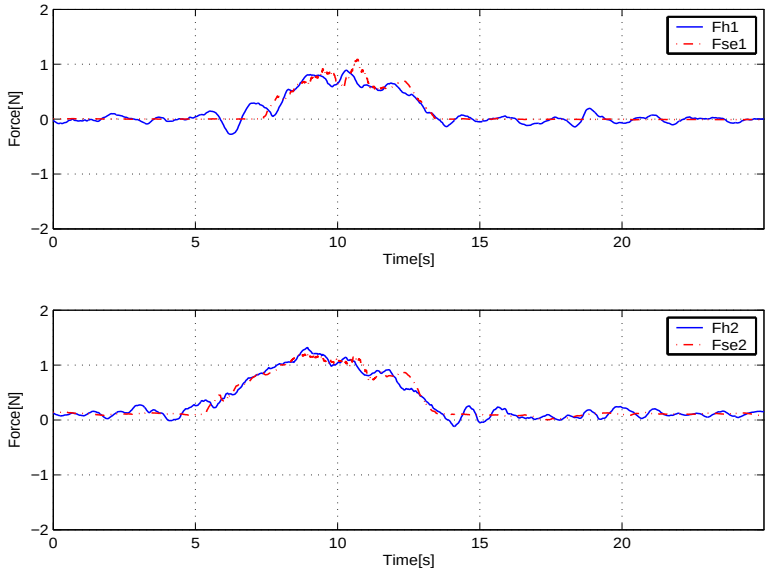

Figure 3.9: Task 1: force profiles with T_d=250 [ms] (Force-Position).

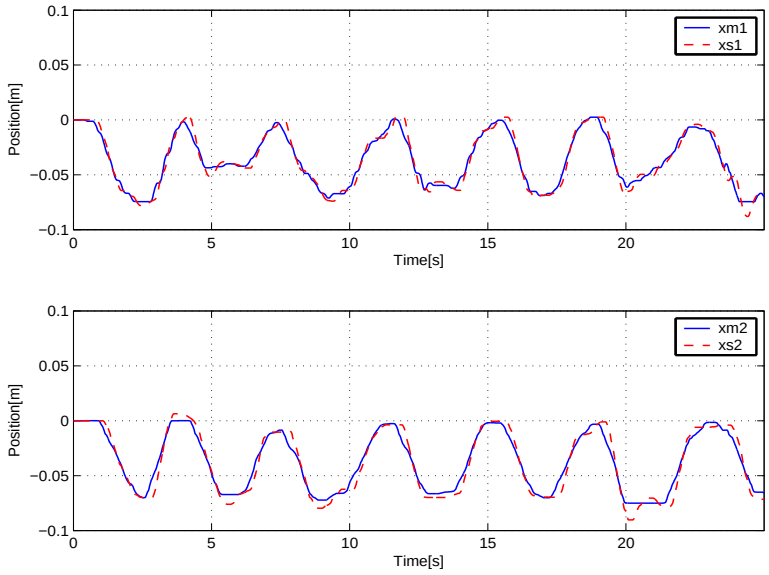

Figure 3.10: Task 1: position profiles with T_d=100 [ms] (Position-Position).

3.2.1 Free motion

To further investigate the transparency of the cooperative teleoperator a free motion test has been perfomed by using the same teleoperator of Fig. 3.1, where the user moves the master devices back and forth applying the forces depicted in Fig. 3.11, Fig. 3.13, Fig. 3.15 and Fig. 3.17 on them. In this test each slave device evolves in free motion following the trajectory of the corresponding master as it is shown in Fig. 3.10, Fig. 3.12, Fig. 3.14 and Fig. 3.16 without contact with the tool. This test confirms that the position tracking performances is satisfactory for both architectures and also for increasing time delays.

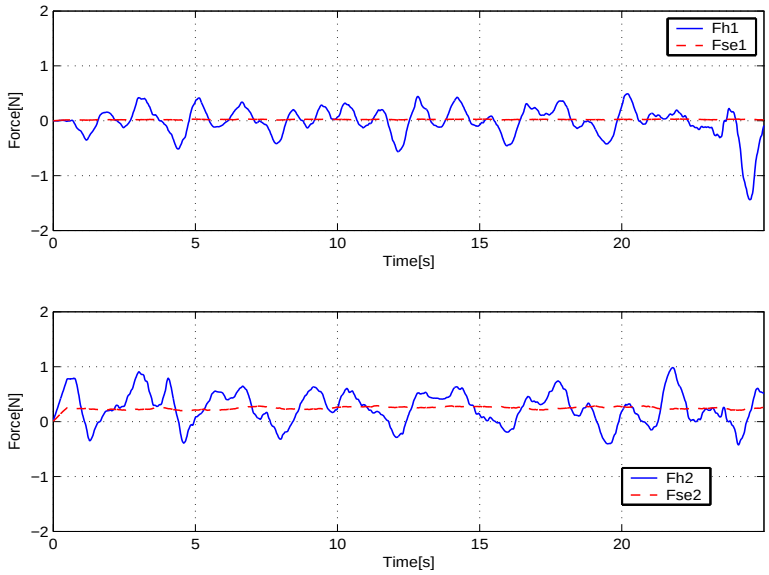

Figure 3.11: Task 1: operator's force profiles with T_d=100 [ms] (Position-Position).

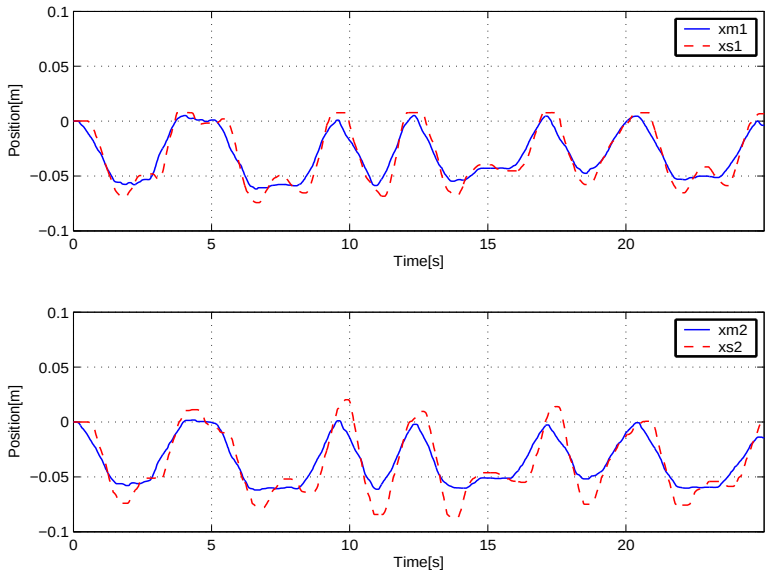

Figure 3.12: Task 1: position profiles with T_d=250 [ms] (Position-Position).

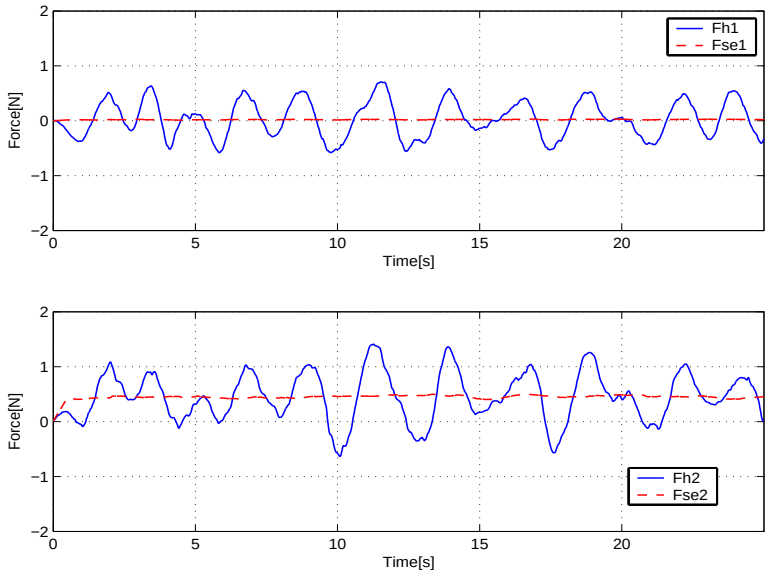

Figure 3.13: Task 1: operator's force profiles with T_d=250 [ms] (Position-Position).

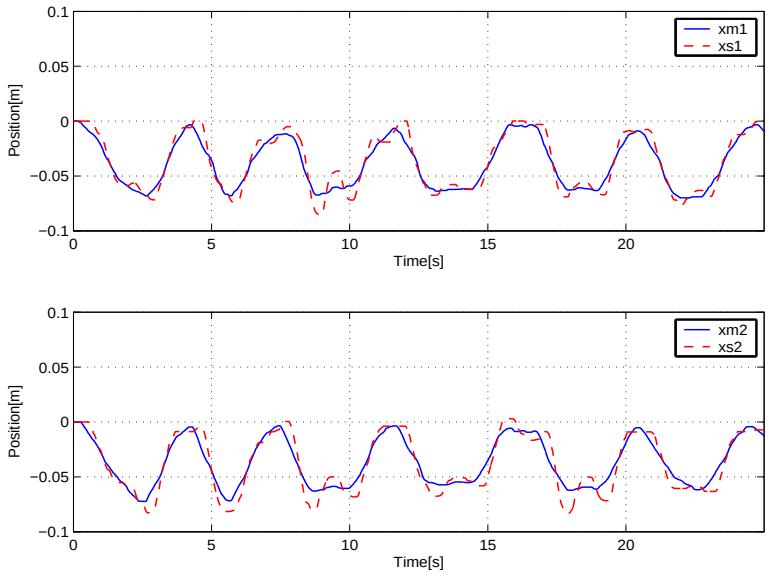

Figure 3.14: Task 1: position profiles with T_d=100 [ms] (Force-Position).

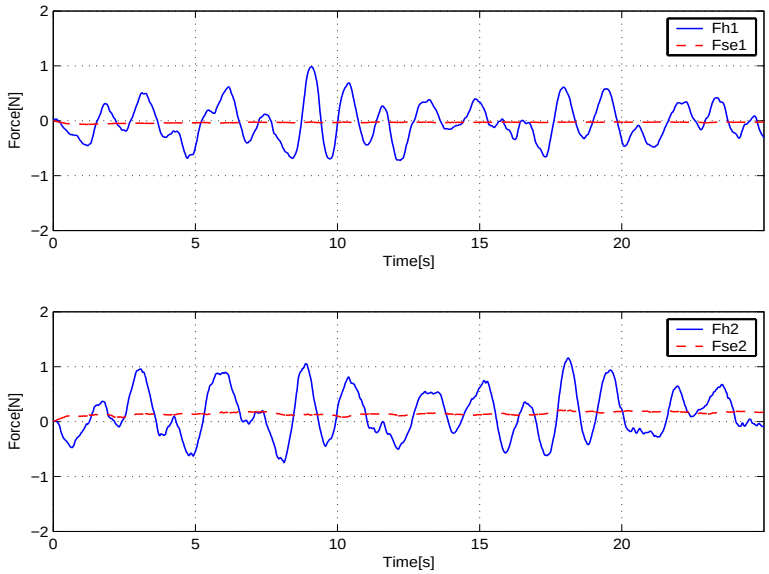

Figure 3.15: Task 1: operator's force profiles with T_d=100 [ms] (Force-Position).

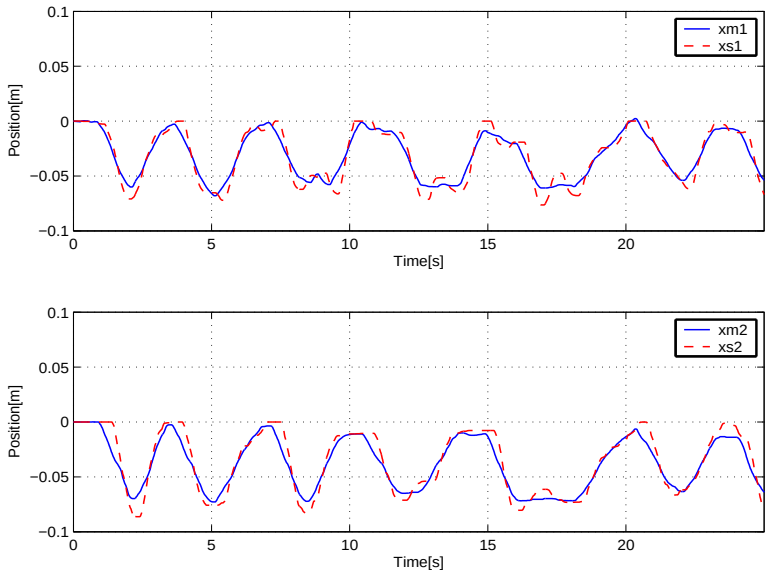

Figure 3.16: Task 1: position profiles with T_d=250 [ms] (Force-Position).

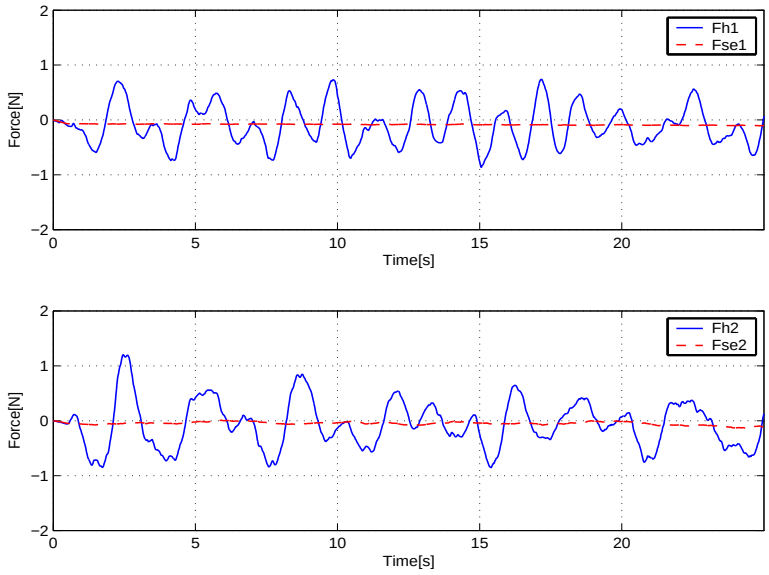

Figure 3.17: Task 1: operator's force profiles with T_d=250 [ms] (Force-Position).

3.3 Handling a common object

In order to excute this task the same cooperative teloperator has been used with the slave motors rotated 180 degrees, see Fig. 3.18. Thus the operator moves the master devices back and forth while the slaves are moved left and right. In this task the two slave manipulators grasp a tool and move it left and right simultaneously. Figures (3.19) and (3.23) show the position profiles of two slave manipulators (red and blue line) and the position of the tool (black), for PP and FP architectures with $T_d = 100[ms]$. As the tool does not have a position sensor, its position profile has been computed as $(xs1 + xs2)/2$. As can be deducted the two cooperative control schemes show good tracking performance. This is also confirmed with increasing time delays see Fig. 3.21 and Fig. 3.25. The Figures (3.20), (3.22), (3.24) and (3.26) illustrate the force profiles exerted by the operator $F_{h1} - F_{h2}$ (blu line) on the master devices and the forces exerted by the slaves on the common tool $F_{se1} - F_{se2}$ (red line).
In all the experimental results the stability is guaranteed even if there are some vibrations in the master-slave position and force profiles. The experimental results validate the simulation results of the previous chapter.

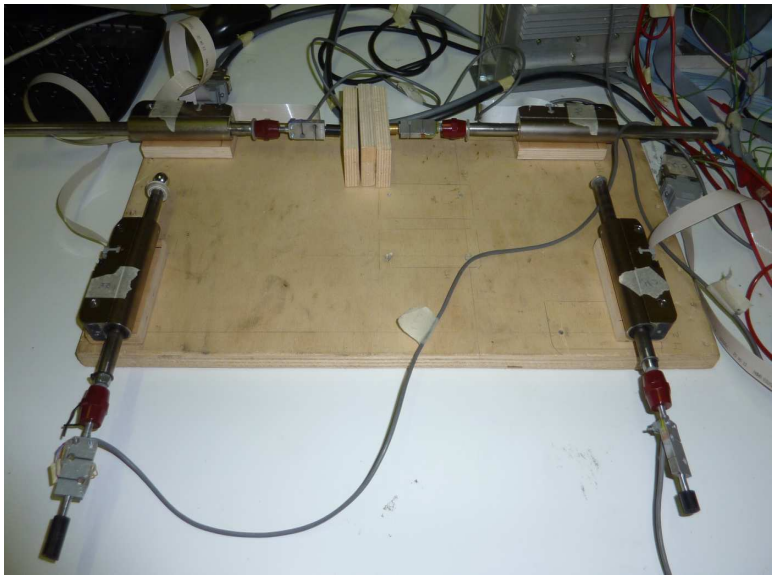

Figure 3.18: Cooperative manipulator, setup to handle a common object.

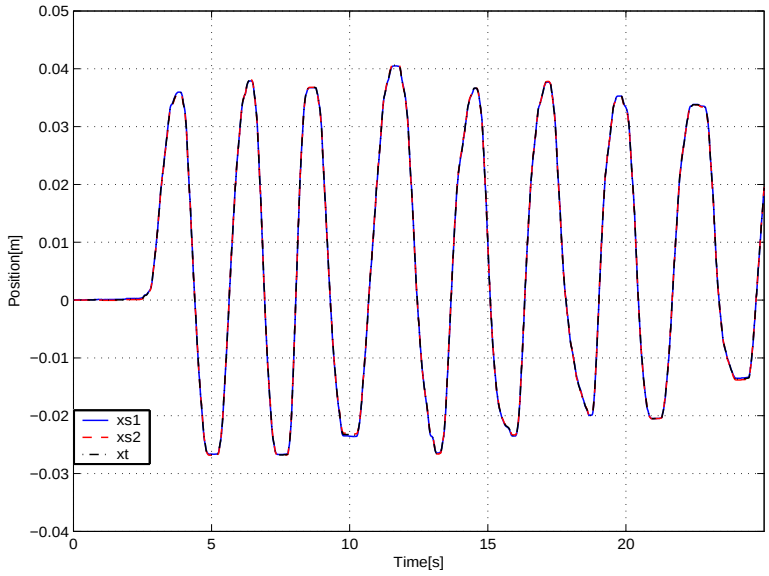

Figure 3.19: Task 2: position profiles with T_d=100 [ms] (Position-Position)

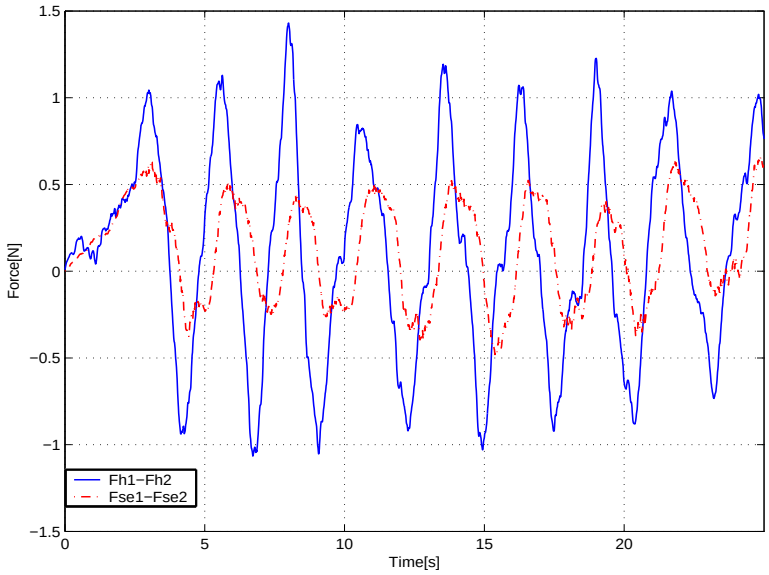

Figure 3.20: Task 2: operator's force profiles with T_d=100 [ms] (Position-Position).

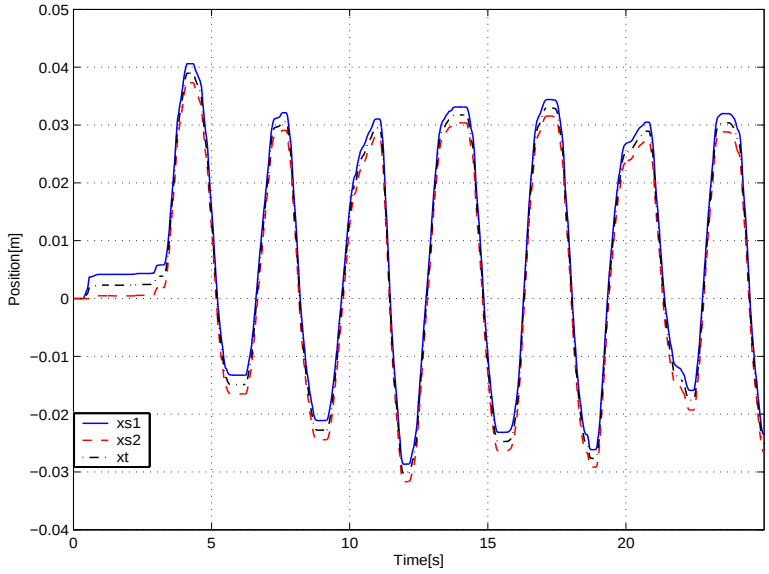

Figure 3.21: Task 2: position profiles with T_d=250 [ms] (Position-Position)

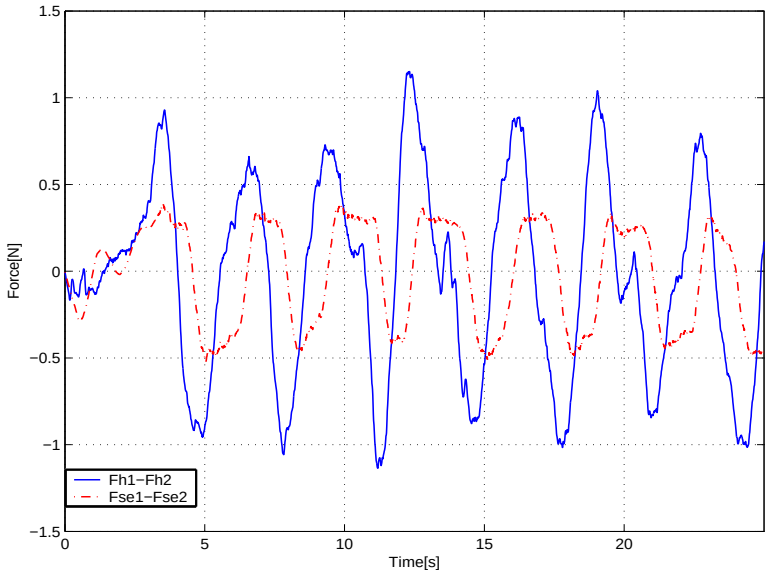

Figure 3.22: Task 2: operator's force profiles with T_d=250 [ms] (Position-Position).

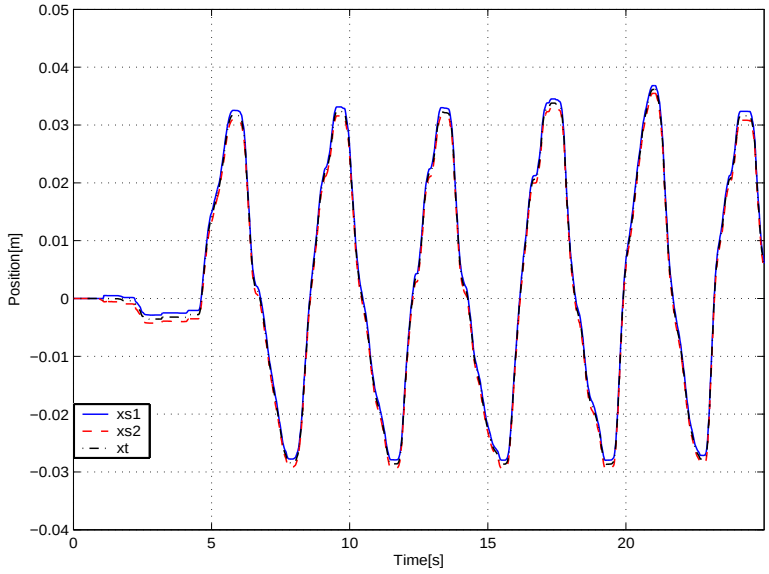

Figure 3.23: Task 2: position profiles with T_d=100 [ms] (Force-Position)

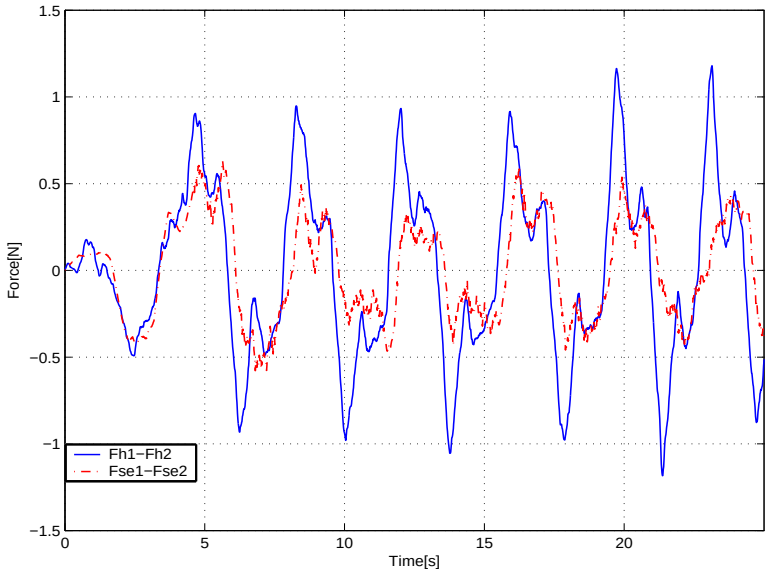

Figure 3.24: Task 2: operator's force profiles with T_d=100 [ms] (Force-Position).

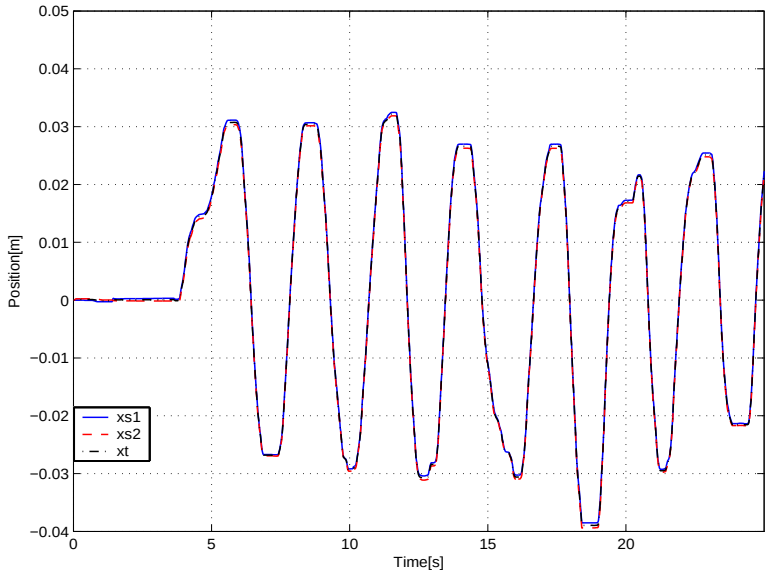

Figure 3.25: Task 2: position profiles with T_d=250 [ms] (Force-Position)

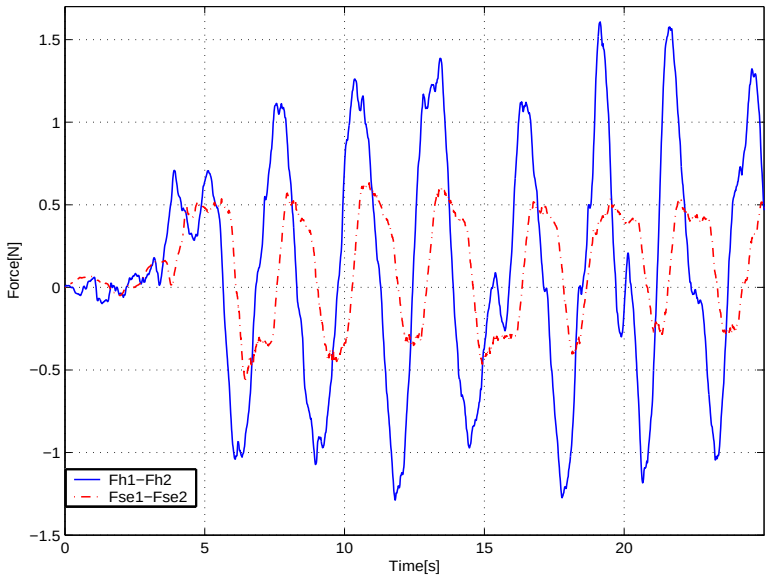

Figure 3.26: Task 2: operator's force profiles with T_d=250 [ms] (Force-Position).

Chapter 4

A Performance and Stability Analysis

This chapter relates to an analysis of the performances of the force-position and the position-position cooperative control schemes, from a transparency and stability point of view by assuming a null time delay in the communication channel.

As it has already been mentioned, the main requirements or goals of a teleoperator system are the trasparency and stability. This chapter firstly adresses a study of trasparency for cooperative teloperation systems and then illustrates an analisys of stability, see [40]. The *transparency* of a teleoperator system is the ability of a teloperator system to present, without any change, the dynamics of the remote environment to the human operator. This goal is unfulfilled because of the presence of the closed-loop dynamics of the master and slave robots which distort the dynamics of the remote environment, see [4], [41], [42]. Since a cooperative teleoperator is composed of more than one teleoperator, the same considerations made for classical ones can be applied for a cooperative one, from a trasparency point of view. Perfect trasparency is unachievable in the master-slave systems, but the trasparency can partially performed depending on the choice of the control architectures employed. Several control architectures have been proposed in the literature of the classical single-master single-slave teleoperator, whose classification is made on the basis of type control on the master and slave device. Chapter 2 illustrates the cooperative control wave-based schemes proposed by the author. This chapter considers the same architecture and defines some parameters which characterize a cooperative system quantitively. These parameters can also provide a criterion to compare different control architectures which support the subjective evaluation of the operator.

4.1 General Description of the System

The control architectures analyzed in this chapter are shown in Fig. 4.1 and Fig. 4.2. They differ with respect to that of Ch. 2 for the lack of time delay. In force-position architecture the exchange of force and position/velocities occurs between each master-slave device. The slave robots try to follow the trajectory imposed by the operator on the master robots, by means of thier PD controllers. The forces exerted from the environment to the slave robots are sent to the master robots and then to the operator. Thus, this scheme requires a force-sensor on the slave side.
In a position-position control scheme the information which travels between the two sides of each teleoperator is the position/velocities of each robot. The position/velocity of each master device is a reference for each slave device which, as in the force-position one, tries to track by means of its own controller. The force feedback, which represents the information about the interaction with the environment, is obtained by means of the Pd controllers of the master robots. In the following, velocity will be used instead of position since the electrical relationship refers to force and velocity (i.e impedance or admittance) even if there are position sensors in a robot and not velocity sensors available for the measurements. In the following, for the sake of simplicity, the equations eq. (2.12), eq. (2.13), eq. (2.14) and eq. (2.15) are rewritten in accordance to the nomenclature of Fig. 4.1 and Fig. 4.2 and assuming the form:

$$M_{mi}\dot{v}_{mi} + B_{mi}\dot{v}_{mi} = F_{mi} \tag{4.1}$$

$$M_{si}\dot{v}_{si} + B_{si}\dot{v}_{si} = F_{si} \tag{4.2}$$

$$F_{mi} = F_{hi} - F_{me_i} \tag{4.3}$$

$$F_{si} = F_{sc_i} - F_{se_i} \tag{4.4}$$

where F_{hi} and F_{se_i} denote respectively, the hand/master interaction force and the slave/environment interaction force, and F_{sc_i} are the control signal computed by the slave controllers.
The values of F_{me_i} depend on the type of control architecture: in the force-position it is equal to F_{se_i}, while in the position-position control scheme it is based on the force computed by the master controller (i.e F_{mc_i} see Fig. 4.2). In Fig. 4.1 and Fig. 4.2 the impedances $Z_{mi}(s) = M_{mi}s + B_{mi}$ and $Z_{si}(s) = M_{si}s + B_{si}$ denote the dynamic characteristics of the master and slave robot respectively, $C_{mi} = (k_{dm}s + k_{pm})/s$ and $C_{si} = (k_{ds}s + k_{ps})/s$ are the PD controllers used at the master and slave side;

In both Fig. 4.1 and Fig. 4.2, the remote side is composed by a shared tool/object M_0, through which the slave manipulators apply forces on the environment, characterized by

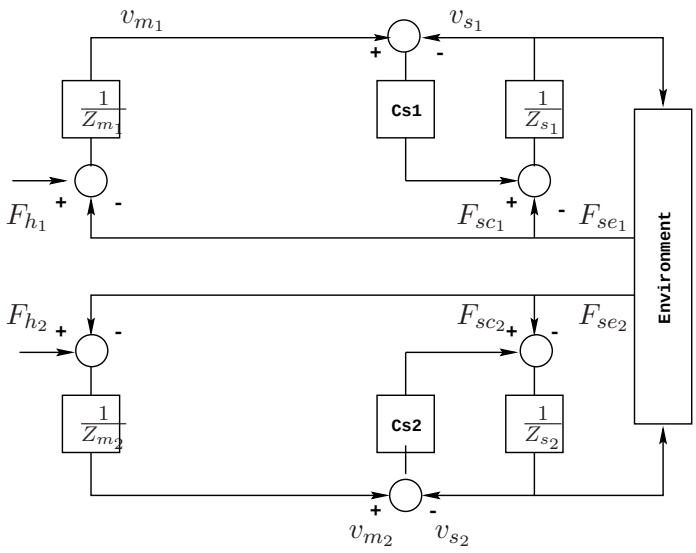

Figure 4.1: Force-Position control architecture.

a stiffness k_e and a damping coefficient b_e as depicted in Fig. 4.3. The dynamics of the tool during interaction with the environment may be described as

$$M_0 \dot{v}_0 = F_{se_1} + F_{se_2} + F_0$$

with

$$F_{se_1} = k_1(x_{s1} - x_0), \qquad F_{se_2} = k_2(x_{s2} - x_0)$$

and

$$F_0 = \begin{cases} -B_e v_0 - K_e(x_o - x_{e_0}) & x_0 \geq x_{e_0} \\ \\ 0 & x_0 \leq x_{e_0} \end{cases} \tag{4.5}$$

where:

- M_0, B_e, K_e are the mass of the tool, and the damping and stiffness coefficients of the environment, respectively;
- F_{se1}, F_{se2} are the forces exchanged at the tool by each slave device;
- F_0 is the force applied by the tool to the remote environment;
- x_{s1} and x_{s2} are the positions of the two slaves;
- v_0 is the velocity of the tool;
- x_{e_0} is the initial position of the environment.

The springs k_1 and k_2 take into account the contact between the slave robots and the common tool (of slave-tool interaction).

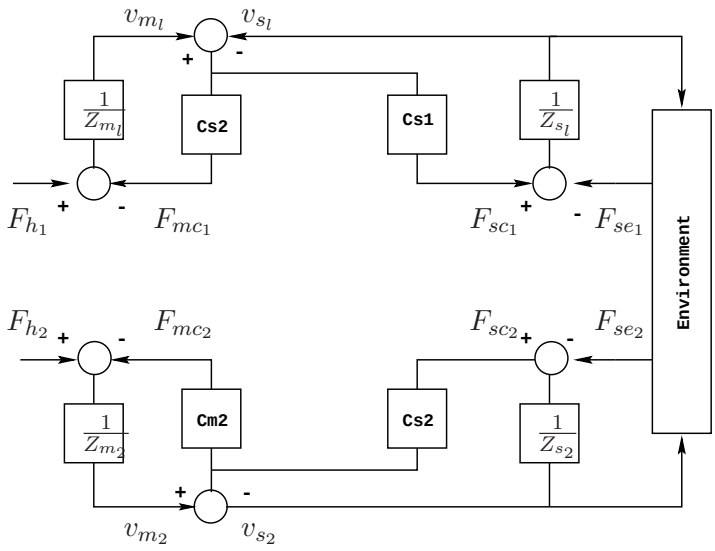

Figure 4.2: Position-Position control architecture.

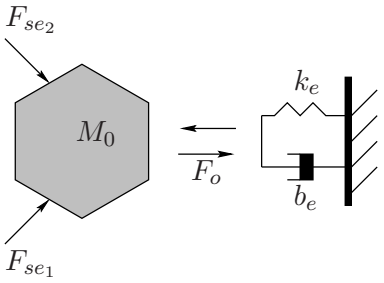

Figure 4.3: Forces applied to the tool.

4.2 Performance metrics

This section analyses the performance metrics of the cooperative systems after a brief summary of the performances of the classical one. A single-master/single-slave teleoperated system, can be analyzed as a two port element, mathematically represented by means of several square matrices, each one of four transfer functions describes the relationships between the forces and the velocities of the two robots. Assuming F_m the hand/master interaction force, F_e the slave/environment interaction force, $\dot{x_m}$ the velocity of the master robot and $\dot{x_s}$ the velocity of the slave robot. It is possible to relate these signals to each other by means of the following matrices:

$$\begin{bmatrix} F_m \\ \\ \dot{x_s} \end{bmatrix} = H \begin{bmatrix} \dot{x_m} \\ \\ F_e \end{bmatrix} \qquad \text{Hybrid parameter matrix} \tag{4.6}$$

$$\begin{bmatrix} \dot{x_m} \\ \\ F_s \end{bmatrix} = G \begin{bmatrix} F_m \\ \\ \dot{x_s} \end{bmatrix} \quad \text{Inverse of Hybrid matrix} \tag{4.7}$$

$$\begin{bmatrix} \dot{x_m} \\ \\ \dot{x_s} \end{bmatrix} = Y \begin{bmatrix} F_m \\ \\ F_e \end{bmatrix} \quad \text{Admittance matrix} \tag{4.8}$$

$$\begin{bmatrix} F_m \\ \\ \dot{x_m} \end{bmatrix} = T \begin{bmatrix} \dot{x_s} \\ \\ F_e \end{bmatrix} \quad \text{Trasmission matrix} \tag{4.9}$$

$$\begin{bmatrix} F_m \\ \\ F_e \end{bmatrix} = Z \begin{bmatrix} \dot{x_m} \\ \\ \dot{x_s} \end{bmatrix} \quad \text{Impedance matrix} \tag{4.10}$$

$$\begin{bmatrix} \dot{x_s} \\ \\ F_s \end{bmatrix} = I \begin{bmatrix} F_m \\ \\ \dot{x_m} \end{bmatrix} \quad \text{Inverse of Trasmission matrix} \tag{4.11}$$

Given the above matrices, proper indices can be computed to compare the performance of the teleoperation systems. Hannaford, see [33], has shown that the hybrid matrix is the most suitable to characterize a teleoperator. The hybrid representation of the master-slave network can be written as

$$\begin{bmatrix} F_m \\ \\ \dot{x_s} \end{bmatrix} = \begin{bmatrix} h_{11}(s) & h_{12}(s) \\ \\ h_{12}(s) & h_{22}(s) \end{bmatrix} \begin{bmatrix} \dot{x}_m \\ \\ F_e \end{bmatrix} \tag{4.12}$$

where:

$$\begin{aligned} h_{11} &= \left.\frac{F_m}{\dot{x}_m}\right|_{F_e=0} \qquad h_{12} = \left.\frac{F_m}{F_e}\right|_{\dot{x}_m=0} \\ h_{21} &= \left.\frac{\dot{x}_s}{\dot{x}_m}\right|_{F_e=0} \qquad h_{12} = \left.\frac{x_s}{F_e}\right|_{\dot{x}_m=0} \end{aligned} \tag{4.13}$$

The mechanical meaning of the parameters represented by equation eq. (4.13) is:

- h_{11} gives the *Impedance in free motion*, i.e. the impedance felt by the operator by moving the master robot with the slave evolving in free motion.
- h_{12} is the *Tracking Force* in contact task, i.e the force encountered by the slave and sent back to the master robot.

- h_{21} is the *Position Tracking*, it represents how well the motion of the slave device follows the motion of the master device.

- h_{22} is the *Contact admittance*, i.e the position tracking in contact task.

For a bilateral system perfect transparency is achieved, see [33], if the hybrid matrix is in the form:

$$H = \begin{bmatrix} 0 & 1 \\ 1 & 0 \end{bmatrix}$$

where 1's refer to the tracking of position and force between the master and the slave devices. The diagonal transfer functions represent the necessary input force to move the master when the slave is contactless and the slave movement for a given slave force, when the master is steady, see [44]. Thus, the 0's mean a null mass and infinite stiffness for the teleoperator and they outline the behavior of a *perfect* teleoperational system from a trasparency point of view. It is also necessary to mention that a perfect teleoperator system is unachievable, above all, due to the presence of the time delay in the communication systems. However, the performance indeces with the above matrix permits the comparison of the performance of the actual teleoperated systems and their control architecture.

As in classical teleoperation, a cooperative system can be mathematically described by means of the relationships which link the forces and velocities of/between each device. Thus, it is also possible to define suitable matrices similar to those shown above for the cooperative systems. They can be expressed as:

$$\begin{bmatrix} F_{h_1} \\ F_{h_2} \\ \dot{x_0} \end{bmatrix} = H \begin{bmatrix} \dot{x_{m_1}} \\ \dot{x_{m_2}} \\ F_0 \end{bmatrix} \qquad \text{Hybrid matrix} \tag{4.14}$$

$$\begin{bmatrix} \dot{x_{m_1}} \\ \dot{x_{m_2}} \\ \dot{x_0} \end{bmatrix} = Y \begin{bmatrix} F_{h_1} \\ F_{h_2} \\ F_0 \end{bmatrix} \qquad \text{Admittance matrix} \tag{4.15}$$

$$\begin{bmatrix} F_{h_1} \\ F_{h_2} \\ \dot{x_{m_1}} \\ \dot{x_{m_2}} \end{bmatrix} = T \begin{bmatrix} \dot{x_0} \\ F_0 \end{bmatrix} \quad \text{Transmission matrix} \tag{4.16}$$

$$\begin{bmatrix} F_{h_1} \\ F_{h_2} \\ F_0 \end{bmatrix} = Z \begin{bmatrix} \dot{x_{m_1}} \\ \dot{x_{m_2}} \\ \dot{x_0} \end{bmatrix} \quad \text{Impedance matrix} \tag{4.17}$$

$$\begin{bmatrix} \dot{x_0} \\ F_0 \end{bmatrix} = I \begin{bmatrix} F_{h_1} \\ F_{h_2} \\ \dot{x_{m_1}} \\ \dot{x_{m_2}} \end{bmatrix} \quad \text{Inverse of Trasmission matrix} \tag{4.18}$$

With any of the previous matrices it is possible to characterise a coooperative system. In the case being studied, the *Hybrid*, *Transmission* and the *Impedance* matrices are considered as they are the most interesting from a physical interpretation.
Regarding the trasparency for a cooperative teleoperators system, we can claim that perfect trsparency is obtained if the hybrid matrix eq. (4.14) is in the form:

$$H = \begin{bmatrix} 0 & 0 & 1 \\ 0 & 0 & 1 \\ 1 & 1 & 0 \end{bmatrix}$$

For the cooperative systems, it seems reasonable to define the performance on the basis of the classical definitions, although proper considerations should be made. For example, in the cooperative systems case at the remote site, besides the remote environment, also the cooperative tool must be considered. Therefore, in the next two subsections the motion/interaction capabilities will be analyzed both with and without the intervening tool.

4.2.1 Performances without the cooperative tool

A cooperative system without the common tool can be simply considered as two separated bilateral teleoperators. Therefore, the hybrid, transmission and impedance matrices in eq. (4.14), eq. (4.16) and eq. (4.18), used in the sequel to compute the performance indices, are defined by:

$$\begin{bmatrix} F_{h_1} \\ F_{h_2} \\ \dot{x_{s_1}} \\ \dot{x_{s_2}} \end{bmatrix} = H \begin{bmatrix} \dot{x_{m_1}} \\ \dot{x_{m_2}} \\ F_{se_1} \\ F_{se_2} \end{bmatrix} \quad \text{Hybrid matrix} \tag{4.19}$$

$$\begin{bmatrix} F_{h_1} \\ F_{h_2} \\ \dot{x_{m_1}} \\ \dot{x_{m_2}} \end{bmatrix} = T \begin{bmatrix} \dot{x_{s_1}} \\ \dot{x_{s_2}} \\ F_{se_1} \\ F_{se_2} \end{bmatrix} \quad \text{Transmission matrix} \tag{4.20}$$

$$\begin{bmatrix} F_{h_1} \\ F_{h_2} \\ \dot{F_{se_1}} \\ \dot{F_{se_2}} \end{bmatrix} = Z \begin{bmatrix} \dot{x_{m_1}} \\ \dot{x_{m_2}} \\ \dot{x_{s_1}} \\ \dot{x_{s_2}} \end{bmatrix} \quad \text{Impedance matrix} \tag{4.21}$$

Since we are in a linear case, the transparency indices for each teleoperator are defined by the transfer functions listed below:

$$h_{11} = \left.\frac{F_{h_1}}{\dot{x}_{m_1}}\right|_{F_{se_1}=0} \qquad h_{21} = \left.\frac{F_{h_2}}{\dot{x}_{m_2}}\right|_{F_{se_2}=0} \tag{4.22}$$

$$h_{31} = \left.\frac{\dot{x}_{s_1}}{\dot{x}_{m_1}}\right|_{F_{se_1}=0} \qquad h_{41} = \left.\frac{\dot{x}_{s_2}}{\dot{x}_{m_2}}\right|_{F_{se_2}=0} \tag{4.23}$$

$$t_{13} = \left.\frac{F_{h_1}}{F_{se_1}}\right|_{\dot{x_{s_1}}=0} \qquad t_{24} = \left.\frac{F_{h_2}}{F_{se_2}}\right|_{\dot{x_{s_2}}=0} \tag{4.24}$$

	Force-Position	Position-Position
Position-tracking	$h_{31} = \frac{C_{s1}}{Z_{cs1}}$ $h_{41} = \frac{C_{s2}}{Z_{cs2}}$	$h_{31} = \frac{C_{s1}}{Z_{cs1}}$ $h_{41} = \frac{C_{s2}}{Z_{cs2}}$
Force-Tracking	$t_{13} = \frac{Z_{m1}}{C_{s1}} + 1$ $t_{24} = \frac{Z_{m2}}{C_{s2}} + 1$	$t_{13} = \frac{Z_{cm1}}{C_{cs1}}$ $t_{24} = \frac{Z_{cm2}}{C_{cs2}}$
Impedance-Free motion	$h_{11} = Z_{m_1}$ $h_{21} = Z_{m_2}$	$h_{11} = Z_{m_1} + \frac{C_{m1}Z_{s_1}}{Z_{cs1}}$ $h_{21} = Z_{m_2} + \frac{C_{m2}Z_{s_2}}{Z_{cs2}}$
Trasmittable-Impedance	$z_{11} = Z_{m1} + C_{s1}$ $z_{21} = Z_{m2} + C_{s2}$	$z_{11} = Z_{cm1}$ $z_{21} = Z_{cm2}$

Table 4.1: Set of parameters for force-position and position-position architectures without the tool.

$$z_{11} = \left.\frac{F_{h_1}}{\dot{x}_{m_1}}\right|_{\dot{x_{s_1}}=0} \qquad z_{12} = \left.\frac{F_{h_2}}{\dot{x}_{m_2}}\right|_{\dot{x_{s_2}}=0} \tag{4.25}$$

The functions in eq. (4.22) and eq. (4.23) refer to the free motion which are determined by imposing the forces F_{se_1} and F_{se_2} equal to zero , acting on each slave device. eq. (4.22) is the impedance in free motion and eq. (4.23) is the position tracking of each teleoperator. On the other hand, eq. (4.24) and eq. (4.25) refer to rigid contact tasks, where the slave devices are considered in a fixed (steady) configuration. eq. (4.24) gives the tracking of force and on the other hand eq. (4.25) represents the maximum transmittable impedance. Please take note that to characterize the contact task, the impedance and transmission parameters have been chosen instead of the hybrid parameters. The reason is that the hybrid parameters in contact task, are obtained with the master robot steady while on the slave robots a force is exerted coming from the environment. This schenario is very difficult to garantee experimentally, thus in the contact task is more reasonable to relate the parameters with the slave steady. In the ideal case both position and force tracking functions should tend towards unity while the impedance in free motion is desired to be as low as possible and the trasmittable impedance should be as large as possible. As an example of the application of these definitions, Tab. 4.1 lists the values of the indices for the force-position and position-position control architectures, where $Z_{cm_i} = Z_{m_i} + C_{m_i}$ and $Z_{cs_i} = Z_{s_i} + C_{s_i}$.

Since the teleoperators are unconnected between themselves, it must be noted that the

cross terms are equal to zero. By looking at the parameters of Tab. 4.1, remarks similar to those for the bilateral architectures can be made. As well known, the tracking performances depend on the choice of the PD controllers and by the relations among them, see [43] for more details.

4.2.2 Performances with the tool

This section analyzes the whole system, considering both the presence of tool and the interaction with the environment. The slave devices considered are always in contact with the tool, and therefore the indices are now related to a contact or non contact task of the tool with the environment. The non-contact situation is associated with the free motion of the tool, while the contact of the tool with the environment can be linked to the rigid contact task of the bilateral systems. For the definition of the performance indices, we refer to the hybrid and transmission matrices in the form described by eq. (4.14) ,eq. (4.16) and eq. (4.18) i.e. considering the object velocity $\dot{x}_0$ and the interaction force F_0 instead of the slave velocities $\dot{x}_{s_1}$, $\dot{x}_{s_2}$, and the corresponding forces F_{se_1} and Fse_2.

The elements (transfer functions) of the hybrid, transmission and impedance matrices have been computed on the basis of the equations of the entire system reported below:

$$\begin{cases} F_{h_1} = Z_{m_1}\dot{x}_{m_1} + F_{mc_1} \\ \dot{x}_{s_1} = \frac{C_{s_1}}{Z_{cs_1}}\dot{x}_{m_1} - \frac{F_{se_1}}{Z_{cs_1}} \\ F_{h_2} = Z_{m_2}\dot{x}_{m_2} + F_{mc_2} \\ \dot{x}_{s_2} = \frac{C_{s_2}}{Z_{cs_2}}\dot{x}_{m_2} - \frac{F_{se_2}}{Z_{cs_2}} \\ Z_0\dot{x_0} = F_{se_1} + F_{se_2} + F_0 \end{cases} \tag{4.26}$$

note that the last equation describes the physical interconnection between the two teleoperators.

Performances with the tool in free motion

These indices describe the behavior of the system when the tool is grasped by each slave device and is not in contact with the environment. This is expressed by imposing the force applied on the environment equal to zero ($F_0 = 0$).

$$h_{31} = \left.\frac{\dot{x_0}}{\dot{x_{m_1}}}\right|_{\dot{x_{m_2}}=0,\ F_0=0} \qquad h_{32} = \left.\frac{\dot{x_0}}{\dot{x_{m_2}}}\right|_{\dot{x_{m_1}}=0,\ F_0=0} \tag{4.27}$$

Equation (4.27) represents the position tracking capabilities of the tool. It permits the understanding and evaluation of the capabilities of the tool to follow the motion of each master device. The impedance in free motion can be added as metric to describe the unconstrained motion, see eq. (4.28). This parameter represents the impedance felt by each operator: its value should be as low as possible and is given as:

	Force - Position
Position - Tracking	$h_{31} = \frac{(Zcs_2 s+k_2)}{d_{fp}}(k_1 C_{s_1})$ $h_{32} = \frac{(Zcs_1 s+k_2)}{d_{fp}}(k_2 C_{s_2})$
Force - Tracking	$t_{12} = \frac{Z_{m_1} Z_{cs_1} s+k_1(Z_{m_1}+C_{s_1})}{C_{s_1} k_1}$ $t_{22} = \frac{Z_{m_2} Z_{cs_2} s+k_2(Z_{m_2}+C_{s_2})}{C_{s_2} k_2}$
Impedance - Free motion	$h_{11} = Z_{m1} + \frac{k_1 C_{s1}}{Z_{cs_1} s+k_1} + hf_{11}$ $h_{22} = Z_{m2} + \frac{k_2 C_{s2}}{Z_{cs_2} s+k_2} + hf_{22}$
Trasmittable - Impedance	$z_{11} = Z_{m_1} + \frac{k_1 C_{s_1}}{Z_{cs_1} s+k_1}$ $z_{22} = Z_{m_2} + \frac{k_2 C_{s_2}}{Z_{cs_2} s+k_2}$

Table 4.2: Set of parameters for force-position architecture with the tool.

$$h_{11} = \left.\frac{F_{m_1}}{\dot{x_{m_1}}}\right|_{\dot{x_{m_2}}=0 \;\; F_0=0} \qquad h_{22} = \left.\frac{F_{m_2}}{\dot{x_{m_2}}}\right|_{\dot{x_{m_1}}=0 \;\; F_0=0} \tag{4.28}$$

Performances with the tool in contact

The case of interaction between the common tool and the remote environment is now considered. In 'classical' bilateral systems, this case is studied by considering the master device when the slave is stopped, see [43]. For the cooperative system under study the performance indices are obtained by keeping the tool in a fixed position in space, i.e. by assuming $\dot{x}_0 = 0$:

$$t_{12} = \left.\frac{F_{h_1}}{F_0}\right|_{\dot{x_0}=0} \qquad t_{22} = \left.\frac{F_{h_2}}{F_0}\right|_{\dot{x_0}=0} \tag{4.29}$$

eq. (4.29) represents the force tracking between the force exerted by the operators and the force applied to the environment. The transfer functions describing the maximum transmittable impedance (from the hybrid matrix) are

$$z_{11} = \left.\frac{F_{h_1}}{\dot{x_{m_1}}}\right|_{\dot{x_0}=0} \qquad z_{22} = \left.\frac{F_{h_2}}{\dot{x_{m_2}}}\right|_{\dot{x_0}=0} \tag{4.30}$$

Tab. 4.2 and Tab. 4.3 report the analytical expressions of the parameters for the two control architectures. In the tables, the following parameters have been used:

	Position - Position
Position - Tracking	$h_{31} = \frac{(Zcs_2 s+k_2)}{d_{fp}}(k_1 C_{s_1})$ $h_{32} = \frac{(Zcs_1 s+k_2)}{d_{fp}}(k_2 C_{s_2})$
Force - Tracking	$t_{12} = \frac{Zcm_1}{C_{s_1}} + \frac{Zcm_1 Z_{cs_1} s}{C_{s_1} k_1} - \frac{C_{m_1} s}{k_1}$ $t_{22} = \frac{Zcm_2}{C_{s_2}} + \frac{Zcm_2 Z_{cs_2} s}{C_{s_2} k_2} - \frac{C_{m_2} s}{k_2}$
Impedance - Free motion	$h_{11} = Z_{mc_1} - \frac{C_{m_1} C_{s_1} s}{Z_{cs_1} s+k_1} - hp_{11}$ $h_{22} = Z_{mc_2} - \frac{C_{m_2} C_{s_2} s}{Z_{cs_2} s+k_2} - hp_{22}$
Trasmittable - Impedance	$z_{11} = Z_{cm_1} - \frac{C_{m_1} C_{s_1} s}{Z_{cs_1} s+k_1}$ $z_{22} = Z_{cm_2} - \frac{C_{m_2} C_{s_2} s}{Z_{cs_2} s+k_2}$

Table 4.3: Set of parameters for Position-Position architecture with the tool.

$$
\begin{aligned}
d_{fp} &= s^2 Z_0 Z_{cs1} Z_{cs2} + s(Z_0 Z_{cs_1} k_2 + Z_0 Z_{cs2} k_1 + \\
&\quad + Z_{cs1} Z_{cs2}(k_1 + k_2)) + (Z_0 + Z_{cs_1} + Z_{cs_2}) k_1 k_2 \\
hf_{11} &= \frac{(-k_1 Z_{cs_1})(Z_{cs_2} s + k_2) k_1 C_{s1}}{d_{fp}(Z_{cs_1} s + k_1)} \\
hf_{22} &= \frac{(-k_2 Z_{cs_2})(Z_{cs_1} s + k_1) k_2 C_{s2}}{d_{fp}(Z_{cs_2} s + k_2)} \\
hp_{11} &= \frac{k_1 C_{m_1}(Z_{cs_2} s + k_2) k_1 C_{s_1}}{(Z_{cs_1} s + k_1) d_{fp}} \\
hp_{22} &= \frac{k_2 C_{m_2}(Z_{cs_1} s + k_1) k_2 C_{s_2}}{(Z_{cs_2} s + k_2) d_{fp}}
\end{aligned}
\tag{4.31}
$$

From the parameters listed in Tab. 4.2 and Tab. 4.3, it is possible to compare the two architectures. The position tracking, as in the bilateral systems, is the same for both architectures since it only depends on the slave devices (which are both under position control). In both architectures, the force tracking depends on the choice of the gains of the PD controllers. This is due to the presence of large values of k_1 and k_2. For the same reason both the impedance in free motion and the maximum transmittable impedance depend on the systems dynamics and on the choice of the control gains.

4.3 Stability Analysis

A stability analysis of the cooperative system is now performed. In the study, the master velocities are considered as input to the system, while the tool velocity is the output. In this case, the cooperative system can be described as:

$$\dot{x}_0 = G_1\dot{x}_{m_1} + G_2\dot{x}_{m_2} \tag{4.32}$$

where $G_1 = \frac{\dot{x}_0}{\dot{x}_{m_1}}|_{\dot{x}_{m_2}=0}$ and $G_2 = \frac{\dot{x}_0}{\dot{x}_{m_2}}|_{\dot{x}_{m_1}=0}$ are defined as:

$$G_1 = \frac{(Zcs_2 s + k_2)}{D(s)}k_1 C_{s_1}, \quad G_2 = \frac{(Zcs_1 s + k_1)}{D(s)}k_2 C_{s_2} \tag{4.33}$$

with

$$\begin{aligned} D(s) &= s^2 Z_0 Z_{cs1} Z_{cs2} + s(Z_0 Z_{cs_1} k_2 + Z_0 Z_{cs2} k_1 + \\ &\quad + Z_{cs1} Z_{cs2}(k_1 + k_2)) + (Z_0 + Z_{cs_1} + Z_{cs_2})k_1 k_2 \end{aligned} \tag{4.34}$$

Therefore, stability is achieved if the characteristic equation of G_1 and G_2 (i.e. $D(s) = 0$) has no positive roots. By substituting the values of Z_0, Z_{cs_1} and Z_{cs_2} in the expression of $D(s)$, one obtains:

$$D(s) = a_6 s^6 + a_5 s^5 + a_4 s^4 + a_3 s^3 + a_2 s^2 + a_1 s + a_0 = 0 \tag{4.35}$$

where:

$$\begin{aligned} a_6 &= M_0 M_1 M_2 \\ a_5 &= M_0[M_1(b_2 + k_{d_2}) + M_2(b_1 + k_{d_1})] \\ a_4 &= M_0(M_1 k_{p2} + M_2 k_{p1}) + M_0(b_1 + k_{d1})(b_2 + k_{d2}) \\ &\quad + M_0(M_1 k_2 + M_2 k_1) + M_1 M_2(k_1 + k_2) \\ a_3 &= M_0[k_{p2}(b_1 + k_{d_1}) + k_{p1}(b_2 + k_{d_2})] + M_0(b_1 + k_{d_1})k_2 \\ &\quad + M_0(b_2 + k_{d_2})k_1 + (k_1 + k_2)[M_2(b_1 + k_{d_1}) + M_1(b_2 + k_{d_2})] \\ a_2 &= M_0(k_{p_1}k_{p_2} + k_{p_1}k_2 + k_{p_2}k_1) \\ &\quad + (k_1 + k_2)[(b_1 + k_{d_1})(b_2 + k_{d_2}) + (M_1 k_{p2} + M_2 k_{p1})] \\ &\quad + k_1 k_2(M_0 + M_1 + M_2) \\ a_1 &= (b_1 + k_{d_1})(k_1 k_{p2} + k_1 k_2 + k_2 k_{p2}) \\ &\quad + (b_2 + k_{d_2})(k_1 k_{p1} + k_2 k_{p1} + k_1 k_2) \\ a_0 &= k_{p_1} k_{p_2}(k_1 + k_2) + (k_{p_1} + k_{p_2})k_1 k_2 \end{aligned}$$

By applying the Routh-Hurwitz criterion to eq. (4.35), the necessary and sufficient conditions for asymptotic stability of the teleoperator are derived as:

$$\begin{aligned}
\Delta_6 &= a_6 > 0 \\
\Delta_5 &= a_5 > 0 \\
\Delta_4 &= \frac{a_5 a_4 - a_6 a_3}{a_5} > 0 \\
\Delta_3 &= a_3 - \frac{a_5(a_5 a_2 - a_1 a_6)}{a_5 a_4 - a_6 a_3} > 0 \\
\Delta_2 &= \frac{a_5 a_2 - a_1 a_6}{a_5} - \frac{a_1(a_5 a_4 - a_6 a_3) - a_0 a_5^2}{a_5^2(a_5 a_4 - a_6 a_3) - a_5^2(a_5 a_2 - a_1 a_6)} > 0 \\
\Delta_1 &= a_1 - \frac{a_0 a_5 a_5}{a_5 a_4 - a_5 a_3} > 0
\end{aligned} \tag{4.36}$$

The stability of the system can be studied also taking into account the presence of the remote environment with impedance Z_e. In this case, the denominator of $G_1(s)$ and $G_2(s)$ in eq. (4.33) is:

$$\begin{aligned}
D(s) = s^2(Z_0 + Z_e)Z_{cs1}Z_{cs2} + s((Z_0 + Z_e)Z_{cs_1}k_2 + (Z_0 + Z_e)Z_{cs2}k_1 \\
+ Z_{cs1}Z_{cs2}(k_1 + k_2)) + ((Z_0 + Z_e) + Z_{cs_1} + Z_{cs_2})k_1 k_2
\end{aligned} \tag{4.37}$$

Again, by substituting the values of Z_0, Z_{cs_1} and Z_{cs_2} and $Z_e = b_e + \frac{k_e}{s}$, one obtains:

$$e_6 s^6 + e_5 s^5 + e_4 s^4 + e_3 s^3 + e_2 s^2 + e_1 s + e_0 = 0 \tag{4.38}$$

where:

$$
\begin{aligned}
e_6 &= M_0 M_1 M_2 \\
e_5 &= M_0[M_1(b_2 + k_{d_2}) + M_2(b_1 + k_{d_1})] + b_e M_1 M_2 \\
e_4 &= M_0[M_1 k_{p2} + M_2 k_{p1} + (b_1 + k_{d_1})(b_2 + k_{d_2})] \\
&\quad + (M_0 M_1 + M_1 M_2)(k_1 + k_2) + k_e M_1 M_2 \\
&\quad + b_e[M_1(b_2 + k_{d_2}) + M_2(b_1 + k_{d_1})] \\
e_3 &= M_0[(k_1 + k_{p1})(b_2 + k_{d_2}) + (k_2 + k_{p2})(b_1 + k_{d_1})] \\
&\quad + M_1[(k_e + k_1 + k_2)(b_2 + k_{d_2}) + b_e k_{p_2} + k_2 b_e] \\
&\quad + M_2[(k_e + k_1 + k_2)(b_1 + k_{d_1}) + b_e k_{p_1} + k_1 b_e] \\
&\quad + b_e(b_1 + k_{d_1})(b_2 + k_{d_2}) \\
e_2 &= M_0(k_{p_1}(k_2 + k_{p_2}) + k_1(k_2 + k_{p_2})) \\
&\quad + M_1(k_e(k_2 + k_{p_2}) + k_1(k_2 + k_{p_2}) + k_1 k_{p_2}) \\
&\quad + M_2(+k_e(k_1 + k_{p_1}) + k_2(k_1 + k_{p_1}) + k_1 k_{p_1}) \\
&\quad + b_e((k_1 + k_{p_1})(b_2 + k_{d_2}) + (k_2 + k_{p_2})(b_1 + k_{d_1})) \\
&\quad + k_e((b_1 + k_{d_1})(b_2 + k_{d_2})) \\
e_1 &= k_e[(k_1 + k_{p_1})(b_2 + k_{d_2}) + (k_{p2} + k_2)(b_1 + k_{d_1})] \\
&\quad + b_e[(k_1 + k_{p_1})(k_2 + k_{p_2})] \\
&\quad + (k_1 + k_2)(k_{p_2}(b_1 + k_{d_1}) + k_{p_1}(b_2 + k_{d_2})) \\
&\quad + k_1 k_2(b_1 + k_{d_1}(b_2 + k_{d_2}) \\
e_0 &= k_e(k_1 + k_{p_1})(k_2 + k_{p_2}) + k_1 k_{p_1}(k_2 + k_{p_2}) + k_2 k_{p_2}(k_1 + k_{p_1})
\end{aligned}
$$

The necessary and sufficient conditions for asymptotic stability of the teleoperator are still given by the conditions eq. (4.36), with the obvious replacement of the parameters a_i with the corresponding e_i, $i = 1, \ldots, 6$. The input/output expressions for the two control schemes are the same, since they only depend on the slave equations, which is under position control in both cases.

Chapter 5

Conclusions

This thesis deals with the study of Coopearative Teleoperation Systems. More precisely, two decentralized control architecture, force-position and position-position, based on wave variables have been proposed and analysed. The architectures have been tested and validated by means of simulation and experimental activities. In both cases two different tasks have been executed which consider the cooperative teleoperator pushing a common object and handling a common object. The simultion results described in Ch. 2 have been obtained using Matlab and Simulink model. They show how both architectures are efficient in terms of performance, measured as position and force tracking, and stability for different time delays. In Ch. 3 the experimental results obtained with a prototype composed by two 1-DOF teleoperator systems are illustred. The experimental results also prove the goodness of the two control schemes. In Ch. 4, by assuming a null time delay, some parameters which characterize quantitively a cooperative systems composed of two pairs of single-master/single-slave devices have been defined. Future activity colud be addressed to deduct the same performance metrics showed in Ch. 4 with the time delays. The topic of this thesis have been published or presented in [31], [36], [40] and [45].

List of Figures

Bibliography

[1] P. Fiorini and R. Oboe *Internet-Based Telerobotics: Problems and Approaches. ICAR '97. 8th Int. Conf. on Advanced Robotics*, Monterey, CA, July 7-9, 1997.

[2] S.Munir and W.J.Book *Control Techniques and Programming Issues for Time Delayed Internet Based Teloperation*, *Journal of Dynamic Systems Measurement and Control-Transactions of the ASME*, Vol. 125, No. 2, pp. 205-214, June 2003.

[3] G. Niemeyer, and J. Slotine, *Towards Force Reflecting Teleoperation over the Internet*, *IEEE International Conference on Robotics and Automation, Leuven, Belgium*, Vol. 3, pp. 1909-1915, May 1998.

[4] D.A. Lawrence, *Stability and Transparency in Bilateral Teleoparation*, *IEEE Trans. on Rob. and Aut.*, Vol. 9(5), p.p. 624-637, Oct. 1993.

[5] S. Hirche, M. Buss, *Human Perceived Trasparency with Time Delay*, *Advances in Telerobotics*, Springer, pp. 191-209, 2007.

[6] R.J. Anderson, and M.W. Spong, *Bilateral Control of Teleoperators with Time Delay*, *IEEE Trans. Automat. Contr.*, AC-34, No. 5, pp. 494-501, May, 1989.

[7] C. Melchiorri, *Robotic Telemanipulation Systems: An Overview on Control Aspects*, Invited Plenary Talk, SYROCO'03, IFAC Symposium on Robot Control, Wroclaw, PL, Sept. 2003.

[8] G. Niemeyer, and J. Slotine, *Stable Adaptive Teleoperation*, *Int. J. Oceanic Engineering*, Vol. 16, No. 1, pp. 152-162, January 1991.

[9] N. Chopra, M. W. Spong, S. Hirche and M. Buss *Bilateral Teleoperation over the Internet: the Time Varying Delay Problem*, *American Control Conference* Vol. 1, pp. 155-160, June 2003.

[10] G. Leung, B. Francis and J. Apkarian, *Bilateral Controller for Teleoperators with Time Delay via mu-Synthesis*, *IEEE Trans. on Rob. and Automat.*, Vol. 2, No. 1, pp. 105-116, Feb. 1995.

[11] H. K. Lee, M. H. Shin and M.J. Chung, *Adaptive Controller of Master-Slave Systems for Trasparent Teleoperation*, *ICAR '97. 8th Int. Conf. on Advanced Robotics.*, pp. 1021-1026, July 1997.

[12] A. Rodriguez, H. Nijmeijer, *Mutual Synchronization of Robots via Estimated State Feedback: A Cooperative Approach*, *IEEE Transactions on Control Systems Technology*, Vol. 12, No. 4, July 2004.

[13] D.Sun and J.K. Mills *Adaptive Synchronized Control for Coordination of Multirobot Assembly Tasks*, *IEEE Transactions on Robotics and Automation*, Vol. 18, No. 4, August 2002.

[14] J.Wang, S.J Dodds and W.N Bailey *Co-ordinated Control of Multiple Robotic Manipulators Handling a Common Object - Theory and Experiments*, *IEEE Proc.-Control Theory Appl.*, Vol. 144, No. 1, January 1997.

[15] R. G. Bonitz and T.C. Hsia *Internal Force-Based Impedance Control for Cooperating Manipulators*, *IEEE Transactions on Robotics and Automation*, Vol. 12, No. 1, February 1996.

[16] S. A. Schneider and R.H. Cannon Jr *Object Impedance Control for Cooperative Manipulation : Theory and Experimental Results*, *IEEE Transactions on Robotics and Automation*, Vol. 8, No. 3, June 1992.

[17] F. Caccavale, P. Chiacchio, A. Marino and L.Villani *Six-DOF Impedance Control of Dual-Arm Cooperative Manipulators*, *IEEE/ASME Transactions on Mechatronics*, Vol. 13, No. 5, October 2008.

[18] R. Garcia-Rodriguez, V. Parra-Vega, *Decentralized Sliding Force/Position PD Control of Cooperative Robots in Operational Space under Jacobian uncertainty Intelligent Robots and Systems*, *IROS 2005. IEEE/RSJ International Conference*, pp. 3726 - 3732, Aug.2005.

[19] S. Sirouspour, *Modeling and Control of Cooperative Teleoperation Systems*, *2005 IEEE Trans. on Rob.*, Vol. 21, pp. 1220-1225, Dec. 2005.

[20] S. Sirouspour, *Multi-operator/Multi-robot Teleoperation: An Adaptive Nonlinear Control Approach*, *IROS 2005. IEEE/RSJ Int. Conf. on Intelligent Robots and Systems.*, pp. 1576-1581, Aug.2005.

[21] S. Sirouspour, *Robust Control Design for Cooperative Teleoperation*, *ICRA 2005. IEEE/RSJ Int. Conf. on Robotics and Automation.*, April.2005.

[22] P. Setoodeh, S. Sirouspour and A. Shahdi, *Discrete-Time Multi-model and Control for Cooperative Teleoperation under Time Delay*, *ICRA 2006. IEEE Int. Conf. on Rob. and Aut. 2006.*, pp. 2921-2926, May. 2006.

[23] I. Elhajj *Design and Analysis of Internet-Based Tele-Coordinated Multi-Robot Systems*, *Auton. Robots*, Vol. 15, pp. 237-254, 2003.

[24] K. Goldberg, B.Chen, R. Solomon, S.Bui, B. Farzin, J.Heitler, D. Poon, G. Smith, *Collaborative Teleoperation via the Internet*, *IEEE Int. Conf. On Rob. and Aut.*, pp. 2019-2024, April 2000.

[25] I. Elhajj, N. Xi, W.K. Fung, Y.H. Liu, Y. Hasegawa, T. Fukuda, *Modeling and Control of Internet Based Cooperative Teleoperation*, *IEEE Int. Conf. On Rob. and Aut.*, Vol.1, pp. 662-667, May 2001.

[26] N.Y. Chong, T. Kotoku, K. Ohba, K.Maeda, N. Matsuhira, K. Tanie, *Development of a Multi-Telerobot System for Remote Collaboration*, *IEEE/RSJ Int. Conf. on Intelligent Robots and Systems.*, Vol. 2, pp. 1002-1007, Nov. 2000.

[27] A. Kheddar, P. Coiffet, Y.Kotoku, K.Tanie *Multi-Robots Teleoperation - Analysis and Prognosis*, *IEEE Int. Workshop on Robot and Human Communication*, pp. 166-171, Sep. 1997.

[28] T.Suzuki, T. Fujii, K. Yokota, H. Asama, H. Kaetsu, I. Endo, *Teleoperation of Multiple Robots through the Internet*, *5th IEEE Int. Workshop on Robot and Human Communication*, pp. 84-89, Nov. 1996.

[29] T.Suzuki, T. Sekine, T. Fujii, H. Asama, I. Endo, *Cooperative Formation among Multiple Mobile Robot Teleoperation in Insoection Task*, *IEEE Int. Workshop on Robot and Human Communication*, pp. 166-171, 1997.

[30] I. Elhajj, A. Goradia, N. Xi, C.M. Kit, Y.H. Liu and T. Fukuda, *Design and Analysis of Internet-Based Tele-Coordinated Multi-Robot Systems*, *Autom. Control*, Vol. 34 No. 5, pp. 494-501, May 1989.

[31] R. Bacocco and C. Melchiorri, *LQ Control Design of Cooperative Teleoperation Systems*, *(ICAR 2009) Int. Conf. on Advanced Robotics*, Munich, July 2009.

[32] J.E. Colgate and N. Hogan, *Robust Control of Dynamically Interacting Systems*, *International Journal of Control*, Vol.48 , No. 1, pp. 65-88, July 1988. *Englewood Cliffs, NJ: Prentice Hall, 1990.*

[33] B. Hannaford, *A Design Framework for Teleoperators with Kinesthetic Feedback*, *IEEE Trans. on Rob. and Automat.*, Vol. 5, pp. 426-434, Aug. 1989.

[34] G. Niemeyer and J.J.E. Slotine and , *Telemanipulation with Time Delays*, *International Journal of Roborics Research*, Vol.23 , No. 9, pp. 873-890, September 2004.

[35] A. Aziminejad, M. Tavakoli, R.V. Patel and M. Moallem *Bilateral Delayed Teleopration: The Effects of a Passivated Channel Model and Force Sensing*, *2007 IEEE Int. Conf. on Rob and Aut.*, pp. 3490-3495, April 2007.

[36] R. Bacocco, G.Borghesan and C. Melchiorri, *Experimental Results for Cooperative Teleoperation Control Schemes*, *CASY Internal Report.*

[37] A. Aziminejad, M. Tavakoli, R.V. Patel and M. Moallem *Enhanced Transparency in Haptics-Based Master-Slave Systems.*, *2007 American Control Conference*, New York City, Usa, July 2007.

[38] A. Aziminejad, M. Tavakoli, R.V. Patel and M. Moallem *Wave-Based Time Delay Compensation in Bilateral Teleoperation: Two Channel versus Four-Channel Architectures.*, *2007 American Control Conference*, New York City, Usa, July 2007.

[39] A. Aziminejad, M. Tavakoli, R.V. Patel and M. Moallem *Transparent Time-Delayed Bilateral Teleoperation Using Wave Variables.*, *IEEE Transaction on Contrl Systems Technology*, Vol. 16, No. 3, May 2008.

[40] R. Bacocco and C. Melchiorri, *A Performance and Stability Analysis for Cooperative Teleoperation Systems*, *(IFAC 2011) 18th IFAC World Congress*, Milan, August 2011.

[41] Y. Yokokohji and T. Yoshikawa, *Bilateral Control of Master-Slave Manipulators for Ideal Kinesthetic Coupling-Formulation and Experiment*, *IEEE Trans. on Rob. and Automat.*, Vol. 10, No. 5, pp. 605-619, 1994.

[42] K. Hashtrudizaad and S.E. Salcudean, *Transparency in Time Delay Systems and the Effect of Local Force Feedback for Trannsparent Teleoperation.*, *IEEE Trans. on Rob. and Automat.*, Vol. 18, No. 1, pp. 108-114, 2002.

[43] I. Aliaga, A. Rubio and E. Snchez, *Experimental Quantitative Comparison of Different Control Architecture for Master-Slave Teleoperation*, *IEEE Trans. on Contr. Sys. Tech.*, Vol. 12, No. 1, Jan. 2004.

[44] J.S. Hart and G. Niemeyer, *Design Guidelines for Wave Variable Controllers in Time Delayed Telerobotics*, *IEEE World Haptic Conference 2007*, pp. 182-187, Tsukuba, Japan, March 2007.

[45] R. Bacocco and C. Melchiorri, *Cooperative Telemanipulation Systems*, *IEEE Telerobotics summer school*, Munich, July 26-30, 2010.

Thanks

ringrazio Alvaro mio faro nella notte ...
..la cooperazione con la geografia...
le donne della mia vita...
....Beatrice e Rachele
tutte le mie amiche..
di cui non riporto i nomi perche' per mia fortuna sono tantissime !!!!
ringrazio Pamela Bartow, my English teacher e co-author dei miei paperi
tutte le Civette del mio Club
tutti miei amici
i mie fratelli transitivi... Daniele e Mario....
...quelli del channel-team
...e quelli del ginetto-team
...quelli che mi hanno adottato all'unibo...
Gianni Borghesan e Riccardo Falconi
ringrazio il mio Prof. Claudio Melchiorri per avermi donato parte della sua conoscenza
e parte della mia autoconsapevolezza.
ringrazio mio papa' e mia mamma ....

...tutti nessuno escluso per il loro affetto !!